

# Positive Hopf plumbed links with maximal signature

Inauguraldissertation

der Philosophisch-naturwissenschaftlichen Fakultät  
der Universität Bern

vorgelegt von

**Lucas Raul Fernández Vilanova**

von Spanien

Leiter der Arbeit:

Prof. Dr. Sebastian Baader

Mathematisches Institut der Universität Bern

This work is licensed under a Creative Commons “Attribution-NonCommercial-NoDerivs 3.0 Unported” license.





# Positive Hopf plumbed links with maximal signature

**Inauguraldissertation**

der Philosophisch-naturwissenschaftlichen Fakultät  
der Universität Bern

vorgelegt von

**Lucas Raul Fernández Vilanova**

von Spanien

Leiter der Arbeit:

Prof. Dr. Sebastian Baader

Mathematisches Institut der Universität Bern

Von der Philosophisch-naturwissenschaftlichen Fakultät angenommen.

Bern, 29. Januar 2021

Der Dekan:

Prof. Dr. Zoltan Balogh



# Contents

<b>Chapter 1</b>	<b>Introduction</b>	<b>1</b>
<b>Chapter 2</b>	<b>Background</b>	<b>7</b>
2.1	Fibred links and Hopf plumbing . . . . .	7
2.1.1	Positive braid links . . . . .	7
2.1.2	Checkerboard graphs links . . . . .	9
2.1.3	Baskets . . . . .	9
2.2	The signature profile . . . . .	10
<b>Chapter 3</b>	<b>Checkerboard graph links and Dynkin diagrams</b>	<b>15</b>
3.1	Introduction . . . . .	15
3.2	Moves on signed graphs . . . . .	17
3.3	Proof of Theorems 3.1 and 3.2 . . . . .	21
3.4	Moves on checkerboard graphs . . . . .	30
<b>Chapter 4</b>	<b>Balloon graphs</b>	<b>35</b>
4.1	Introduction . . . . .	35
4.2	Balloon graphs . . . . .	36
4.3	Proof of Proposition 4.1 . . . . .	38
4.4	Linear time algorithm . . . . .	42
4.5	E7 graphs . . . . .	43
<b>Chapter 5</b>	<b>Checkerboard graph links and baskets</b>	<b>47</b>
<b>Chapter 6</b>	<b>Baskets and fibred links realizing <math>A_n</math></b>	<b>51</b>
6.1	Introduction . . . . .	51
6.2	A note on $A_n$ graphs . . . . .	52
6.3	Proof of Theorem 6.1. . . . .	53
6.4	Plumbing on a basket . . . . .	55
	<b>Bibliography</b>	<b>59</b>



## Acknowledgements

First of all, my foremost appreciation goes to my advisor Sebastian Baader. In the course of the four-year study, he not only provided me with professional academic support, but also his expertise, together with the enthusiasm and perseverance in mathematics, inspired and stimulated me to acquire this achievement.

Furthermore, I would like to express my gratitude to Pierre for reviewing this thesis.

Special thanks also go to: Livio L. for the beneficial advise and feedback; Lukas, for the valuable discussions about checkerboard graph moves; Arthur, for the patient explanations on root systems; Filip, for the profitable talks about plumbing; Ian, for the informative introduction to the basket links and the inspiring talks about checkerboard graphs; and Levi, for the enlightening talks about the linear graph algorithm.

In addition, I am very thankful to Arthur, Livio Ferreti and Plinio. They kindly offered help and support in diverse manners besides my academia life and enriched my experience in Bern with engaging adventures. Moreover, I am appreciative to Yinuo, in every sense.

Last but not least, I gratefully acknowledge the constant support from Susana, Luis and Jorge in all aspects.





# Chapter 1

## Introduction

A Hopf band is an annulus embedded in  $\mathbb{R}^3$  with a full twist. If the twist is positive, we say that the Hopf band is positive and negative otherwise. An important property of the boundary of a Hopf band is that it is a fibred link, which means that the complement is endowed with a fibre bundle over  $S^1$ . Fibred links were first defined by Stallings in 1961, [31], and they are the main object of study in this thesis. We can create more intricate surfaces using an operation called plumbing, defined by Stallings who showed that plumbing two fibre surfaces yields a fibre surface [32]. Giroux and Goodman later showed that any fibred surface can be obtained by a sequence of plumbing and de-plumbing (the reverse operation) Hopf bands [18]. A quick way to see this operation is to choose a proper arc in each Hopf band or surface, then glue its corresponding neighbourhoods transversely in such a way that the two bands are contained in complementary half-spaces. It is possible to choose an arc that goes along the Hopf band  $n$  times, obtaining an even more complicated surface (unless there are only two Hopf bands), like the one in Figure 1, in which we plumb a third band that goes twice around the first one. In such cases, the core curves of the Hopf bands may intersect multiple times. We will give more examples of this in the next section. This thesis is focused on the links arising by positive Hopf plumbing such that core curves intersect no more than once.

The signature of a link,  $L$ , is a topological invariant found by Trotter [34] and commonly denoted by  $\sigma(L)$ . Let  $V$  be a Seifert matrix of  $L$ , then  $\sigma(L)$  can be calculated by finding the signature of the symmetrized Seifert matrix of the link  $(V + V^T)$ . The signature is maximal when the matrix is a positive (or negative) definite. Another interesting invariant is the signature function (defined in [23] and [33] by Levine and Tristram), which can be constructed by calculating the signature of the Hermitian matrix  $(1 - w)V + (1 - \bar{w})V^T$  for different values of the complex number  $w \in S^1$ . This thesis is concerned mostly with the first invariant, but we will glimpse the latter in the next chapter, where we find the signature function for certain types of positive Hopf plumbed links.

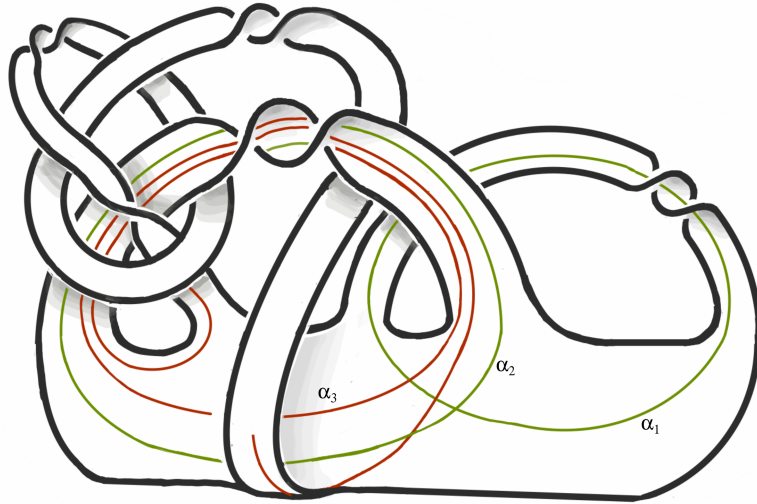


Figure 1.1: An example of three positive Hopf bands plumbed together. Note that the core curve  $\alpha_3$  intersects twice  $\alpha_1$ . For simplicity  $\alpha_3$  is not fully drawn.

The symmetric Seifert matrices have the form of 2's in the diagonal and 0 or  $\pm 1$  otherwise. From the algebraic point of view, it is known that these positive definite matrices are congruent to one of the Cartan matrices or direct sums of the simply laced Dynkin diagrams:  $A_n$ ,  $D_n$ ,  $E_6$ ,  $E_7$  and  $E_8$ , see Figure 1.2. We will denote them by *ADE* diagrams. These diagrams have been widely studied in connection with the classification of semi-simple Lie algebras and in the context of graph theory where the Cartan matrix is written in terms of the adjacency matrix [9], [10]. When plumbing positive Hopf bands according to these graphs we get the torus links  $T(2, n+1)$ ,  $T(3, 4)$  and  $T(3, 5)$  for  $A_n$ ,  $E_6$  and  $E_8$ , respectively, and the pretzel links  $P(-2, 2, n-2)$  and  $P(-2, 3, 4)$  for  $D_n$  and  $E_7$  respectively, [7]. An example of  $T(2, n+1)$  is in Figure 6.1. We will use the notation  $L(G)$  when referring to the link realized by the graph  $G$ , as suggested in [7].

The goal of this thesis is to classify links with a maximal signature within a certain class of fibred links into one of the links realized by the *ADE* diagrams. A similar study was carried out by Boileau, Boyer and Gordon [6] showing that for strongly quasipositive links to have an L-space cyclic branched cover, they need to have a maximal signature, and more recently they showed that certain strongly quasipositive braids with a definite closure can be classified into the links realized by the *ADE* diagrams.

We will differentiate plumbings in which the core curves of the Hopf bands intersect at most once and those in which they can intersect more than once. In the latter, Misev found that for such constructions, there is an infinite family of distinct fibred knots having the same Seifert form as the torus knots  $T(2, 2g+1)$  for any given genus  $g \geq 2$ , [26]. That is why, from now on, we will consider plumb-

ings of the former type.

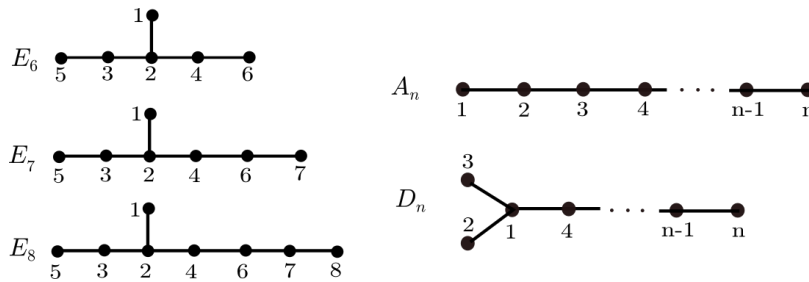


Figure 1.2: The simply laced Dynkin diagrams.

We begin with the positive braid links, a class of links that has been studied in the context of singularity theory, which can be constructed by plumbing positive Hopf bands; see Figure 1.3 for the example of the positive trefoil link or check [16] for more enlightening figures. Baader [1] showed that a prime positive braid with maximal signature is isotopic to one of the  $ADE$  links. The proof involved braid relations, conjugation and a list of graph minors.

**Theorem 1.1.** ([1, Theorem 2]) *A prime positive braid with maximal signature is isotopic to one of the links realized by the  $ADE$  diagrams.*

It is customary to represent positive braid links with a linking graph, the construction of which consists of associating each Hopf band to a vertex, and such that two vertices are connected whenever the corresponding core curves of the Hopf bands intersect. Baader, Lukas and Liechti [3] not only showed that linking graphs uniquely determines a positive braid link, but also built the basis to construct a new class of links, which generalizes the previous ones, and uniquely determines a strongly quasipositive fibred link. These were called checkerboard graph links. One of the most noticeable differences between checkerboard graphs and linking graphs is that the former has no restriction on the valency of the vertices.

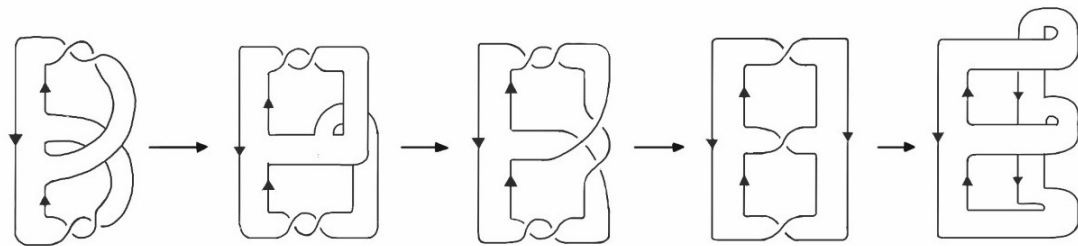


Figure 1.3

Our first result (see Chapter 3) was to show that the *ADE* classification extends to checkerboard graph links. The proof uses the same list of graph minors used in [1], and a set of moves on the checkerboard graph that preserves the link type. These moves, which we call triangle- or *t*-moves have appeared before in graph theory and were known as local switching [10]. Here, we use a restricted set of those to prove the following theorem.

**Theorem 3.3.** *A checkerboard graph link with maximal signature is isotopic to one of the links realized by the ADE diagrams.*

The next class of links, which includes positive braid links, are called basket links and were introduced by Rudolph [30]. Their construction consists of plumbing Hopf bands onto a disk in a given order. They can be represented by what is known as a chord diagram [20]. The kind of *freedom* when plumbing Hopf bands in such a manner breaks down the *ADE* classification. Examples of basket links that were not  $L(D_n)$  but had a Seifert form of type  $D_n$  (we will refer to them as ‘fake’) were found by Boileau et al. [7], Theorem 1.13. This result and the previous theorem show that not all baskets are checkerboard graph links. It remains an open question as to whether baskets are a generalization of checkerboard graph links. We explore this question in Chapter 5.

**Conjecture 5.1.** *Checkerboard graph links are basket links.*

Using Boileau et al.’s Theorems 1.13 and 9.10 it is not difficult to show that such *fake* knots can also be found for  $E_{6,7,8}$ . However, our result shows that no fake  $A_n$  type basket links exist.

**Theorem 6.1.** *A basket link with  $n$  positive Hopf bands and symmetrized Seifert form congruent to  $C_{A_n}$  is isotopic to a two-strand torus link.*

In the more general class of links where plumbing positive Hopf bands only have the restriction that core curves intersect at most once, we found that there were links with the same Seifert form as  $A_n$  but different from the torus links  $T(2, n + 1)$ , (see the anticipated example in Figure 1.4). This shows the limits of the *ADE* classification for this type of fibred links. Both results are discussed in Chapter 6.

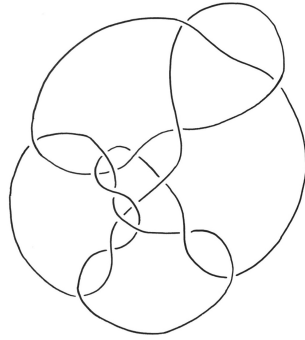


Figure 1.4: A 17-crossings fibred knot resulting from plumbing 6 positive Hopf bands. It has the same Seifert form as  $T(2,7)$  yet they are not isotopic. Images plotted with *knotscape* [21].

The *fake*  $A_n$  links are interesting given the recent conjecture [7] stating that fibred strongly quasipositive links such that its cyclic branched cover is an L-space are *simply laced arborescent*, e.g., of the type  $T(2, n + 1)$ . Secondly, these examples also become interesting in the context of the prevailing slice-ribbon conjecture, since Baker proved that if  $K$  and  $K'$  are two distinct fibred strongly quasipositive knots, then  $K \# -K'$  is not ribbon, [4]. Although we show that the two-component links ( $n$  odd) that we produce are not smoothly concordant to  $T(2, n + 1)$ , for  $n$  even, we do not know if our knot is concordant to  $T(2, n + 1)$ .

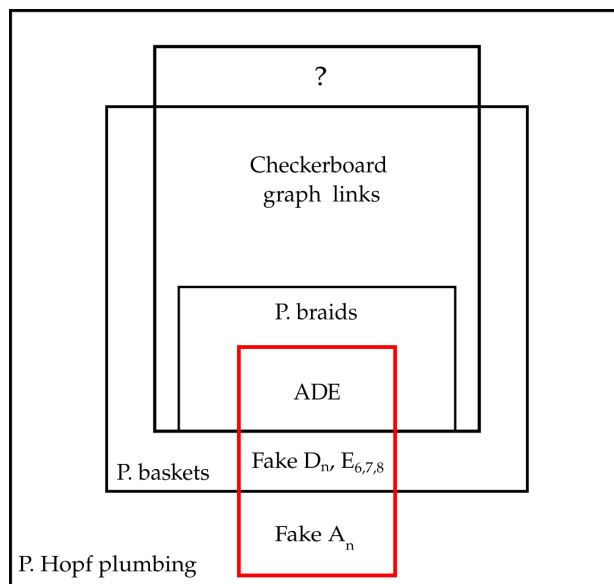


Figure 1.5: A summary of the links constructed by plumbing positive Hopf bands, in such a way that the core curves intersect at most once. The red square represents the ones with maximal signature. The question mark is a reference to Conjecture 5.1.

A characterization of two-strand torus links in terms of linking graphs was given in [2] and dubbed *triangle tree graphs*. They proved the existence of a linear time algorithm for detecting the torus links  $T(2, n + 1)$  out of a positive braid. In Chapter 4 we complete the study of checkerboard graph links with maximal signature by giving a new characterization in terms of checkerboard graphs of the pretzel links  $P(-2, 2, n - 2)$ .

**Proposition 4.1.** *Let  $\Gamma$  be a checkerboard graph with  $n$  vertices and  $L(\Gamma)$  the associated link. Then,  $L(\Gamma)$  is isotopic to  $L(D_n)$  if and only if  $\Gamma$  is either a 1-balloon graph or one of the three types of graphs in Figure 4.1 below, where the dashed circles represent triangle tree graphs.*

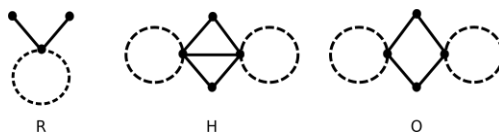


Figure 1.6: The underlying graphs of type  $R$ ,  $H$  and  $O$ . The triangle tree graph in  $R$  must contain at least one edge.

To prove Proposition 4.1 we make use of the list of minors used in Theorem 3.3, and the set of  $t$ -moves. In addition, we provide a list of checkerboard graphs such that their corresponding links are isotopic to  $L(E_6)$  or  $L(E_7)$ . Finally, we also found that there exists a linear time algorithm in the number of vertices plus the number of edges to detect  $L(D_n)$  from a checkerboard graph.

**Theorem 4.7.** *There exists an algorithm linear in  $E + V$  to detect checkerboard graph links with maximal signature from a checkerboard graph.*

**Outline:** In Chapter 2 we give the definitions and examples of the main links under study in this thesis: positive braids links, checkerboard graph links and basket links. We also define the signature function of a link and compute it for the cases of three and four positive Hopf bands plumbed together. In particular, we investigate the behaviour of the signature function when the intersection of the core curves of these Hopf bands goes to infinity. In Chapter 3, we define the  $t$ -moves for checkerboard graphs and use them to prove Theorem 3.3. In Chapter 4, we continue the study of checkerboard graphs of maximal signature. We characterize those whose corresponding link is of the  $ADE$  type, and use this to show that there is a linear time algorithm to find these links from a checkerboard graph. In Chapter 5 we explain Conjecture 5.1 and prove some partial results. In Chapter 6 we prove Theorem 6.1 and provide some examples of fake  $A_n$  links.

# Chapter 2

## Background

### 2.1 Fibred links and Hopf plumbing

Let  $S$  be a Seifert surface of a link  $L$ . In this thesis we assume that links and Seifert surfaces are smooth, compact, oriented and embedded in  $S^3$ . We say that  $L$  is a fibred link if  $S$  is a fibred surface, i.e., there exists a fibre bundle with base and total space  $S^1$  and  $S^3 - L$ , respectively. Pictorial examples of the fibred bundle of a trefoil knot and the unknot can be found in [29]. A fibred surface comes with a map  $h : S \rightarrow S$  called the monodromy, which fixes the boundary pointwise, and is a very strong tool when studying fibred links. We refer the reader to [29] for an introduction to knot theory, fibred links and monodromy maps.

Plumbing Hopf bands is a special case of an operation known as Murasugi sum [27]. Here, we will go directly to the definition of plumbing Hopf bands as it was defined by Stallings [32]. Let  $\Sigma_1$  be a fibred surface and  $H_2$  a Hopf band, define two proper arcs  $\alpha_1 \subset \Sigma_1$  and  $\alpha_2 \subset H_2$  and discs  $D_{\alpha_1}, D_{\alpha_2}$  to be the corresponding neighborhoods of the arcs. Now, glue  $\partial D_{\alpha_1}$  and  $\partial D_{\alpha_2}$  transversely in such a way that the two bands are contained in complementary half-spaces.

In the following sections we give a short insight into three types of fibred links constructed by plumbing positive Hopf bands: positive braid links, checkerboard graph links, and basket links.

#### 2.1.1 Positive braid links

Let  $B_n$  be the braid group on  $n$  strands (also known as the Artin braid group), an element in this group can be written as a finite product of the standard generators  $\sigma_1, \dots, \sigma_{n-1}$  and their inverses. Now, a positive braid word is one in which no inverses of the generators are allowed, and the closure is known as a positive braid link. For instance,  $L(A_n)$  is the closure of  $\sigma_1^n$ , and in Figure 2.1, we show the

fibred surface associated with the closure of the positive braid  $\sigma_2^2(\sigma_1\sigma_3\sigma_2\sigma_4)^2$ . A result due to Stallings shows that the closure of a positive braid word is fibred and can be constructed by positive Hopf plumbing [32].

When it comes to represent a positive braid link (apart from using a braid word), we can do so by using what are called brick diagrams, which are a special case of fence diagrams, the latter were defined by Rudolph as a way of representing a more general class of links named *strongly quasipositive links*. A brick diagram, as its name suggests, can be constructed by changing each crossing in a positive braid by an horizontal line. Although we do not give a precise example of these, in Figure 2.1, left, the red blocks form the brick diagram of the given positive braid link. They represent a natural homology basis of the surface. Another representation, which will be extensively used in this thesis, consists in associating each brick to a vertex and joining two vertices whenever the corresponding homology elements of the bricks intersect. The result is an oriented, planar, finite and simple graph with maximum valency 6, called linking graph. Remarkably, in [3] it is proven that a linking graph uniquely determines a positive braid link.

We adopt the convention used in [3], there, “vertical” edges are oriented downwards and all other edges are oriented upwards. This assures that adjacent cycles have different orientation. Moreover, the orientation of the edge  $e_{i,j}$  give us the sign of the linking number of the corresponding homology bases of the vertices  $v_i$  and  $v_j$ . This motivates the following definition:

**Definition 2.2:** *A signed graph is a finite and simple graph in which every edge is assigned a value 1 or -1.*

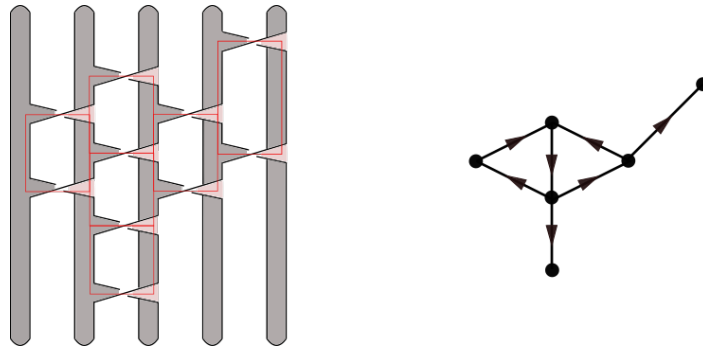


Figure 2.1: An example of the Seifert surface of  $\sigma_2^2(\sigma_1\sigma_3\sigma_2\sigma_4)^2$  and the corresponding linking graph. The red curves represent a natural homology basis. Note that they are in one-to-one correspondence with the vertices of the linking graph and two vertices are joined by an edge if the corresponding elements of the basis intersect.

Let  $G$  be a signed graph and  $A(G)$  be its adjacency matrix (where  $A(G)_{ij} = \pm 1$  if the vertices  $i$  and  $j$  are connected by an edge). Now, let  $\beta$  be a positive braid word and  $\Gamma(\beta)$  be its linking graph, then there exists a signed graph  $\Gamma^\pm(\beta)$  such



that  $2I + A(\Gamma^\pm(\beta))$  is the symmetrized Seifert form of the closure of  $\beta$ , which we will denote as  $L(\Gamma(\beta))$ , (Proposition 1.4.2, [16]). Clearly, the underlying graph of  $\Gamma(\beta)$ , which we will denote as  $|\Gamma(\beta)|$ , is the same as  $|\Gamma^\pm(\beta)|$ .

### 2.1.2 Checkerboard graphs links

A checkerboard graph is a generalization of a linking graph. They are finite, simple, plane and oriented graphs whose cycles are coherently oriented. The latter property is equivalent to saying that they admit a checkerboard coloring, i.e., their dual, without the vertex corresponding to the *unbounded* face, is a bipartite graph. The interest of studying these graphs resides in the fact that a checkerboard graph uniquely determines a strongly quasipositive fibred link [3, Theorem 2]. How to recover a checkerboard graph link from a checkerboard graph is explained in [3].

In addition, as showed in [3] it is possible to associate to a checkerboard graph an abstract open book i.e., a pair  $(\Sigma, \phi)$ , where  $\Sigma$  is an oriented compact surface with boundary, and  $\phi$  is a diffeomorphism, called the monodromy, that fixes the boundary pointwise. Baader and Lewark use the open books realized by checkerboard graphs in order to find two moves on these graphs that preserve the corresponding link type [2], such moves will be of importance in the proof of Theorem 3.3, and are a special case of the  $t'$ -moves defined in Chapter 3.

For positive braid knots the topological 4-genus is maximal exactly if the signature is maximal [24]. Whether it is possible to obtain the same result for checkerboard graph links is a question proposed by [3].

### 2.1.3 Baskets

Basket links were first defined by Rudolph [30]. They are strongly quasipositive fibred links, that include positive braid links. They are constructed by plumbing Hopf bands along the neighborhoods of properly embedded arcs in a disk. The easiest and more intuitive representation of a basket as it appears in [20], is by using the so called chord diagrams; a disk in  $\mathbb{R}^2$  with ordered chords, see for instance Figure 2.2, left. From there, we can build the basket surface by plumbing Hopf bands in the given order and following the convention of plumbing the  $i^{th}$  band on bottom of the previous bands, see Figure 2.2, right.

The incidence graph,  $\Gamma$ , of a chord diagram has one vertex for each chord and such that two vertices are connected whenever the corresponding chords intersect, e.g, Figure 2.2 (left) is a chord diagram with incidence graph  $A_3$ . It is worth mentioning that, looking at Figure 2.2 (right), if we change a bottom plumbing by a top plumbing, the basket surface does not change [30]. There are incidence graphs, e.g,  $A_n$ , where the order in which we plumb is irrelevant. In fact, in [20] it is shown that this is also true for tree graphs.

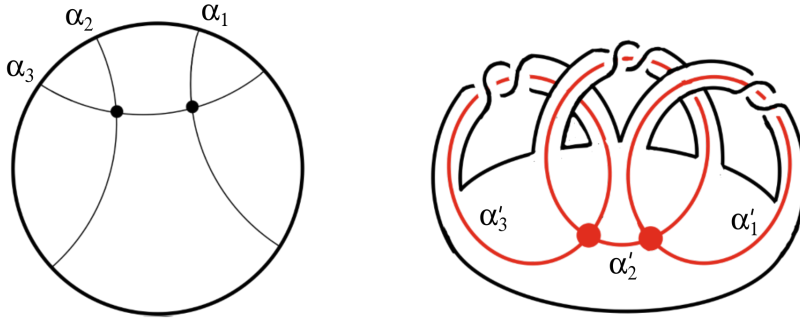


Figure 2.2: A chord diagram, left, and its basket surface, right.

A chord diagram with arcs  $\alpha_1, \dots, \alpha_n$  together with an order of plumbing determines uniquely a signed graph,  $\Gamma^\pm$ . We obtain  $\Gamma^\pm$  as follows: identically as we did with the incidence graph we associate one vertex for each arc and one edge whenever two arcs intersect. In order to find the sign, let  $\alpha'_i$  be the oriented core curve of the positive Hopf band plumbed along  $\alpha_i$ , then the sign of the edge  $[\alpha_i, \alpha_j]$  is given by the sign of  $lk(\alpha'_i, \alpha'_j) + lk(\alpha'_i, \alpha'_j)$ , where  $\alpha'_i$  is the curve resulting from pushing  $\alpha'_i$  off in the positive normal direction of the surface. Clearly, the incidence graph is the underlying graph of  $\Gamma^\pm$ . Moreover, in this basis, the basket surface has symmetrized Seifert matrix  $M(\Gamma^\pm) = 2I + A(\Gamma^\pm)$ . In Chapter 6, we consider basket links whose symmetrized Seifert matrix is congruent to the Cartan matrix of  $A_n$ , which can be written as:

$$C_{A_n} = \begin{pmatrix} 2 & -1 & & & & \\ -1 & 2 & -1 & & & \\ & -1 & 2 & -1 & & \\ & & & \ddots & & \\ & & & & -1 & 2 & -1 \\ & & & & & -1 & 2 \end{pmatrix}.$$

This is a positive definite matrix, so if  $M(\Gamma^\pm) \cong C_{A_n}$  then so is  $M(\Gamma^\pm)$  and the eigenvalues of  $A(\Gamma^\pm)$  are  $> -2$ . This is why, in order to prove Theorem 6.1, we use some of the results of spectral graph theory, in which they study precisely the signed graphs whose eigenvalues are greater than  $-2$ .

## 2.2 The signature profile

To each link  $L \subset S^3$ , there is associated a signature function (defined in [23] and [33]), which can be constructed by calculating the signature of the Hermitian matrix  $M_w$  for different values of the complex number  $w \in S^1$ . Here,

$$M_w = (1 - w)V + (1 - \bar{w})V^T$$

where  $V$  is a Seifert matrix for  $L$ . Let  $S \subset S^3$  be the fibre surface obtained by plumbing  $n$  positive Hopf bands  $H_1, \dots, H_n$  with oriented core curves  $\alpha_1, \dots, \alpha_n$ , and let  $m_{ij}$  be the geometric intersection number between the core curves  $\alpha_i$  and  $\alpha_j$  for  $i \neq j$ . We can find a symmetrized Seifert matrix with twos in the diagonal (the self-linking of the bands) and  $\pm m_{ij}$  otherwise, where the sign depends on the orientation of the core curves.

We are interested on what kind of signature function can be realized from the link  $L = \partial S$  if we make the intersection numbers between the core curves tend to infinity, more precisely, we study whether in this case there is a finite or infinite number of signature profiles. Our first result is the following:

**Proposition 2.1:** *There are only two types of signature profiles for a link obtained by plumbing three positive Hopf bands, and an infinite number of signature profiles if obtained by plumbing four positive Hopf bands.*

*Proof:* We will start with the case of three Hopf bands. Let  $S \subset S^3$  be the fibre surface obtained by plumbing three positive Hopf bands  $H_1, H_2, H_3$  with core curves  $\alpha_1, \alpha_2, \alpha_3$  respectively. We want to construct a Seifert matrix for  $S$ . If we plumb the first two Hopf bands  $H_1$  and  $H_2$  together, it is not difficult to see that the intersection number between their core curves is always  $\pm 1$  or 0. Let us choose the orientation of  $\alpha_1$  and  $\alpha_2$  so that  $lk(\alpha_1, \alpha_2) = -1$ . Now, plumb a third band,  $H_3$ , so that the geometric intersection number between  $\alpha_1$  and  $\alpha_3$  is  $n \geq 0$  and between  $\alpha_2$  and  $\alpha_3$  is  $m \geq 0$ . Note that there is only one way of orienting  $\alpha_3$ , so it agrees with the previous two bands, it follows that  $lk(\alpha_1, \alpha_3) = n$  and  $lk(\alpha_2, \alpha_3) = -m$  (or equivalently  $lk(\alpha_1, \alpha_3) = -n$  and  $lk(\alpha_2, \alpha_3) = m$ ), and a Seifert matrix  $V$  of the surface  $S$  can be written as

$$V = \begin{bmatrix} 1 & -1 & n \\ 0 & 1 & -m \\ 0 & 0 & 1 \end{bmatrix}.$$

Let  $M_w$  be an Hermitian matrix of  $V$  where  $w = e^{i\pi x}$  and  $x \in [0, 1]$ . In this proof we calculate the signature of  $M_w$  as described by Macduffe [4], by subtracting the number of sign changes to the number of sign permanences of the principal minors of  $M_w$ .

In order to simplify the calculus denote  $B = (1 - w)$ ,  $\bar{B} = (1 - \bar{w})$  and  $A = 2(1 - \cos(x))$ . From our notation, it is not difficult to obtain the identities  $B\bar{B} = A$  and  $\bar{B} + B = A$ , so the matrix  $M_w$  of  $V$  is

$$M_w = \begin{bmatrix} A & -B & nB \\ -\bar{B} & A & -mB \\ \bar{B}n & -m\bar{B} & A \end{bmatrix}.$$

Now, we can easily compute the principal minors of  $M_w$ , denote them by  $M_i$  with  $i = 1, 2, 3$ . Then,

$$M_1 = A, \quad M_2 = A^2 - A, \quad M_3 = A^3 - A^2(n^2 + m^2 + 1 - nm).$$

Note that,  $n^2 + m^2 + 1 - nm > 0$ , and all values are realized by finitely many pairs  $(n, m) \in \mathbb{Z}^2$ , in particular the values 1, 2 and 3. These are the values where the minor  $M_3$  has a root between 0 and  $\pi$ . Make the substitution  $A = 2(1 - \cos(x))$ , now we want to evaluate the sign of the minors for different values of  $x \in [0, \pi]$ . Note that if  $x = 0$  then  $M_i = 0$  for all  $i$ .

The first two expressions are not hard to analyse:  $M_1 > 0$  for all  $x \in (0, \pi]$ ;  $M_2$  has one root at  $\delta_2 = \pi/3$ , taking negative values for  $x < \delta_2$  and positive values otherwise. Now, if  $m$  and  $n$  takes the values  $(0, 1)$ ,  $(1, 0)$  or  $(1, 1)$  then  $M_3$  has one root at  $\delta_3$  such that  $\delta_3 > \delta_2$  and it takes negative values for  $x < \delta_3$  and positive ones otherwise. In the cases that  $m, n > 1$  or  $m = 0$  and  $n > 1$  (or equivalently  $n = 0, m > 1$ ) then  $M_3$  has no roots in  $(0, \pi]$  and takes negative values in that interval.

Define  $\{1, \text{sgn}(M_1), \dots, \text{sgn}(M_3)\}$  to be the sequence of signs of the principal minors for a given value of  $x$  and recall that the signature of  $M_w$  is equal to number of sign changes minus the number of sign permanences in this sequence [4]. Thus, we can construct two types of signature profiles: first, if  $m$  and  $n$  takes the values  $(0, 1)$ ,  $(1, 0)$  or  $(1, 1)$  we obtain the sign sequences  $\{1, +, -, -\}$  if  $x \in (0, \delta_2)$  and  $\{1, +, +, -\}$  if  $x \in (\delta_2, \delta_3)$  giving a signature equal to 1 in both cases, and if  $x \geq \delta_3$  then  $\{1, +, +, +\}$  with signature equal to 3, see Figure 2.3 (bottom). Now, if  $m, n > 1$  or  $m = 0$  and  $n > 1$ , then  $\{1, +, -, -\}$  for  $x \in (0, \delta_2)$  and  $\{1, +, +, -\}$  if  $x > \delta_2$  both cases have signature 1, see Figure 2.3 (top).  $\square$

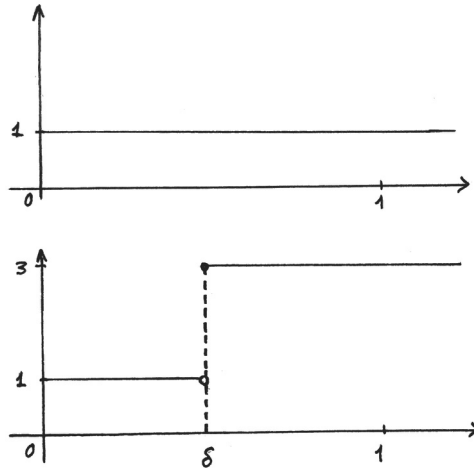


Figure 2.3: Top: signature function where  $m$  and  $n$  takes the values  $(0, 1)$ ,  $(1, 0)$  or  $(1, 1)$ . Bottom: signature function for  $m, n > 1$  or  $m = 0$  and  $n > 1$ .

Now, let's consider the case of four positive Hopf bands. Let  $S \subset S^3$  be the fibre surface obtained by plumbing four positive Hopf bands, let  $V$  be a Seifert matrix for  $S$  and  $m$  be the intersection number between two of the core curves of the bands. We calculate the signature function of  $S$  for different values of  $m$ , in a similar manner as we did in the previous section. We show that when  $m$  tends to infinity there is an infinite number of signature profiles; one for each value of  $m$ . Consider,

$$V = \begin{bmatrix} 1 & -1 & 0 & 1 \\ 0 & 1 & -1 & m \\ 0 & 0 & 1 & 1 \\ 0 & 0 & 0 & 1 \end{bmatrix}.$$

Let  $M_w(V)$  be the Hermitian matrix of  $V$  as defined before, and let  $M_i$  for  $i = 1, 2, 3, 4$  be its principal minors,

$$M_1 = A, \quad M_2 = A^2 - A, \quad M_3 = A^3 - 2A^2, \quad M_4 = A^4 - (5 + m^2)A^3 + 4A^2.$$

Note that the first three minors are the same as in the previous section (for the case  $m = 1$  and  $n = 0$ ), and they do not depend on  $m$ . The real roots for  $M_4$  in  $x \in (0, \pi]$  are

$$A = \frac{1}{2}(m^2 \pm \sqrt{m^4 + 10m^2 + 9 + 5}).$$

Thus,

$$x_1 = 2\pi k + \arccos\left(1 - \frac{1}{4}(m^2 - \sqrt{m^4 + 10m^2 + 9 + 5})\right)$$

for  $k \in \mathbb{Z}$ , is one of the real roots after the substitution  $A = 2(1 - \cos(x))$ . Here,  $x_1$  tends to zero as  $m$  goes to infinity and  $M_4$  takes positive values for  $x < x_1$  and negative ones otherwise. Therefore, the sign sequence for  $x < x_1$  is  $\{1, +, -, -, +\}$  which has signature 0 and for  $x > x_1$  it is not hard to see that the sign sequences gives a signature of 2 in the three possible intervals:  $(x_1, \delta_2)$  with sequence  $\{1, +, -, -, -\}$ ,  $(\delta_2, \delta_3)$  with  $\{1, +, +, -, -\}$  and  $(\delta_3, \infty)$  with  $\{1, +, +, +, -\}$ . Since the signature function has a discontinuity at  $x_1$ , this represents a jump, which tends to zero as  $m$  goes to infinity.  $\square$



## Chapter 3

# Checkerboard graph links and Dynkin diagrams

In this chapter we define an equivalence relation on graphs with signed edges, such that the associated adjacency matrices of two equivalent graphs are congruent over  $\mathbb{Z}$ . We show that signed graphs whose eigenvalues are larger than  $-2$  are equivalent to one of the simply laced Dynkin diagrams:  $A_n$ ,  $D_n$ ,  $E_6$ ,  $E_7$  and  $E_8$ . We use the previous result to prove that a checkerboard graph link with maximal signature is isotopic to one of the links realized by the simply laced Dynkin diagrams.

### 3.1 Introduction

Let  $G$  be a signed graph, we say that  $G$  is a positive signed graph if  $2I + A(G)$  is positive definite. For such graphs, we define a  $t$ -move that transforms one graph into another such that their adjacency matrices are congruent. This defines an equivalence relation that we call a  $t$ -equivalence.

**Theorem 3.1.** *Let  $G$  be a positive signed graph, then  $G$  is  $t$ -equivalent to one of the  $ADE$  diagrams.*

A wide research in the field of spectral graph theory has been carried out on the graphs whose adjacency matrix have eigenvalues  $> -2$ . Results from Cameron et al. [9] characterize those graphs *represented* by one of the  $ADE$  root systems. It is worth mentioning that a similar conclusion to the one in Theorem 3.1 can be achieved by using their results. However, the advantage of using the  $t$ -moves lies in the fact that, as we will further explain in Section 3.4, they are in close connection with certain checkerboard graph moves that preserve the link type.

If we only consider signed graphs that are planar and admit a checkerboard coloring (we shall call those graphs signed checkerboard graphs), we will find that

Theorem 3.1 can be slightly sharpened. Indeed, we only need to use certain types of  $t$ -moves, which we call the  $t'$ -moves. We say that two graphs are  $t'$ -equivalent if there is a sequence of such moves relating one to another. Section 3.2 provides a concise introduction to the  $t$ - and  $t'$ - moves on signed graphs and we give some of their properties.

**Theorem 3.2.** *Let  $G$  be a positive signed checkerboard graph, then  $G$  is  $t'$ -equivalent to one of the  $ADE$  diagrams.*

In Section 3.3 we will prove Theorems 3.1 and 3.2 by induction on the number of vertices. We show that if we add a vertex to one of the  $ADE$  diagrams, we obtain a graph that is either  $t'$ -equivalent to one of the  $ADE$  diagrams, or it has a non-positive Seifert form. To show the latter, we make use of the forbidden minors  $E$ ,  $T$ ,  $X$  and  $Y$ , which do not have a positive definite symmetrized Seifert form, independently of their signs [1]. Figure 3.1 shows the unsigned minors. In addition, we include the  $\tilde{D}$  graph in our list of minors that have a positive semidefinite symmetrized Seifert form. A key step in the proof is that moves on unsigned graphs can be promoted to moves on signed graphs; therefore, simplifying the proof considerably.

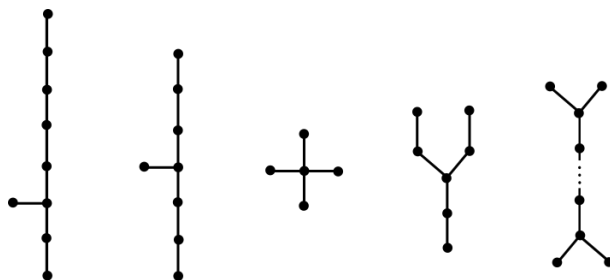


Figure 3.1: Forbidden minors, reading from left to right:  $E$ ,  $T$ ,  $X$ ,  $Y$  and  $\tilde{D}$ . Any signed graph containing an induced subgraph of these five types has a non-positive Seifert form.

Finally, in Section 3.4 we slightly generalize the moves proposed in [2] to find a version of the  $t'$ - moves for checkerboard graphs. We also explain the relation between sign graphs and checkerboard graphs, and we prove Theorem 3.3:

**Theorem 3.3.** *A checkerboard graph link with maximal signature is isotopic to one of the links realized by the  $ADE$  diagrams.*



## 3.2 Moves on signed graphs

We dedicate this section to define what we call a  $t$ -move on a signed graph, as well as the  $t'$ -moves, which are special cases of the former ones. Along that, we also study some of their properties that will be of importance in order to prove Theorems 3.1. and 3.2.

Before going into definitions, we discuss two three of detecting non-positive graphs aside from the forbidden minors mentioned above. Note that the latter are extremely useful when dealing with tree graphs, where signs can be ignored; however, once we encounter a cycle, the signs are important. Indeed, the following remarks show that the number of vertices and the number of negative edges in a cycle play a crucial role for detecting non-positive graphs.

**Remark 3.4.** Suppose  $G$  is an  $n$ -cycle graph with  $x$  number of negative edges and  $n \geq 3$ . Let  $A(G)$  be its adjacency matrix. It is clear that if we change the signs of the two incident edges of a vertex in  $G$ , then the corresponding adjacency matrices are congruent. If the number of negative edges is even, we can transform the cycle into one with only positive edges, otherwise we can reduce the number of negative signs to one. Then, after a permutation of rows and columns

$$2I + A(G) \cong \begin{pmatrix} 2 & 1 & & & \pm 1 \\ 1 & 2 & 1 & & \\ & 1 & 2 & 1 & \\ & & & \ddots & \\ & & & 1 & 2 & 1 \\ \pm 1 & & & & 1 & 2 \end{pmatrix}.$$

Where  $\cong$  denotes matrix congruence over  $\mathbb{Z}$ . Here the entries  $(1, n)$  and  $(n, 1)$  are positive if  $x$  is even and negative otherwise. The determinant of the principal minor  $(2I + A(G))_{n-a}$  is  $n - a + 1$  for  $1 \leq a \leq n - 1$ . Hence, to determine whether  $2I + A(G)$  is positive definite, it suffices to study its determinant. Using the co-factor expansion it is not hard to check that  $\det(2I + A(G)) = 0$  if  $x$  and  $n$  have the same parity and  $\det(2I + A(G)) = 4$  otherwise.

When the number of negative edges and the number of vertices in a cycle have different parity we say that the cycle is positive. Remark 3.4 establishes a necessary condition for a signed graph with cycles to be positive, namely, there is an odd number of positive edges.

**Remark 3.5.** Let  $\Theta$  be a graph consisting of two positive cycles sharing  $x \geq 2$  edges,  $t$  of which are negative. Let  $(n, p)$  and  $(m, q)$  be these two cycles, where  $n$  and  $m$  are the number of vertices and  $p, q$  stand for the number of negative signs in each cycle. Then, the *outer cycle* is an induced subgraph with  $m + n - 2x$  edges

and  $p + q - 2t$  of them are negative. Since the pairs  $n, p$  and  $m, q$  have different parity, it follows that the *outer cycle* is not positive. Therefore, two positive cycles sharing more than one edge form a non-positive graph. Note that in the case for  $x = 1$  there is not such an induced subgraph.

**Remark 3.6.** Consider the graph in Figure 3.2, where  $A$ ,  $B$  and  $D$  represent positive cycles of lengths  $\geq 3$ . The outer cycle, as an induced subgraph, is not a positive graph. The proof is similar to that in Remark 3.5.

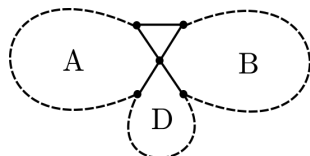


Figure 3.2

We are now ready to define a  $t$ -move for signed graphs in three steps. Let  $G$  be a signed graph, the cycles of which are positive:

**Step 1.** Pick any edge  $\epsilon(x, y)$  in  $G$ , where  $\epsilon \in \{1, -1\}$  is the sign of the edge, and choose one of its endpoints, say  $x$ .

**Step 2.** Let  $\{v_1, \dots, v_n\}$  be the set of vertices adjacent to  $y$  (excluding  $x$ ). In the case  $x$  is the only adjacent vertex, jump directly to Step 3. Now, for all  $v_i \in \{v_1, \dots, v_n\}$  draw an edge from  $x$  to every vertex  $v_i$ , with the same sign as the edge  $(y, v_i)$  if  $\epsilon = -1$  and opposite sign if  $\epsilon = 1$ . If an edge already exists, remove it.

**Step 3.** Change  $\epsilon$  by  $-\epsilon$ .

We say that two signed graphs  $G_1$  and  $G_2$  are  $t$ -equivalent, and we denote it by  $G_1 \sim G_2$ , if there exists a sequence of  $t$ -moves changing  $G_1$  into  $G_2$ . Sometimes we write the pair  $[v, w]$  to indicate that we perform a  $t$ -move on the edge  $(v, w)$  and vertex  $v$ .



Figure 3.3: An example of a  $t$ -move on the vertex and edge marked with a circle where the dashed lines indicate negative edges.

Let  $G$  be a signed graph and  $|G|$  the graph we obtain from  $G$  by ignoring the signs of its edges, this is usually called the underlying graph of  $G$ , a name that we adopt in this paper. Observe that the underlying graph of a signed graph that results from a  $t$ -move on  $G$  does not depend on the signs of the edges in  $G$ . So

it is possible to define the  $t$ -move for non-signed graphs (by simply ignoring edge signs in steps 1 and 2 and skipping step 3).

**Remark 3.7.** It is easy to verify that if we have a signed graph  $G$  and a sequence of  $t$ -moves on  $|G|$  such that  $|G| \sim |G'|$ , then the same sequence (choosing the same edges and vertices) transforms  $G$  into  $G'$ , where the signs of  $G'$  depend on those in  $G$  and the chosen sequence.

Since we will consider forbidden minors that are trees and we are interested on sequences that lead to tree graphs and the signs in a tree does not matter (see Remark 3.4); henceforth, we will consider underlying graphs only. This includes figures, starting at Figure 3.4.

For later use, consider the graph in Figure 3.4 (left side), which we call a B graph. It is not hard to check that:



Figure 3.4: Graph B.

Similarly, one can check the following relations:

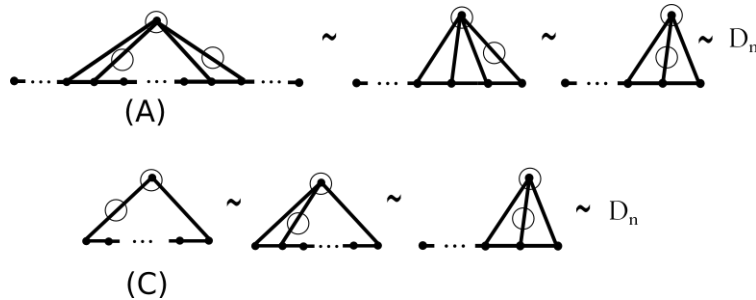


Figure 3.5: The graphs (A) and (C) are  $t$ -equivalent to  $D_n$ .

The graphs  $B$ ,  $A$  and  $C$  are not only an instructive example, but they will also be useful in the proof of Proposition 3.1.

**Lemma 3.8.** Let  $G_1$  be a signed graph the cycles of which are positive and let  $G_2$  be a signed graph. If  $G_1 \sim G_2$ , then  $2I + A(G_1) \cong 2I + A(G_2)$ .

*Proof:* Consider the vertex  $v_j$  and the edge  $(v_i, v_j)$  with sign  $\epsilon$  in  $G_1$ . The matrix  $2I + A(G_1)$  has the form

$$\begin{pmatrix} & & & \vdots & \vdots & & \\ & & & a_{mi} & a_{mj} & & \\ & & & \vdots & \vdots & & \\ \dots & a_{im} & \dots & 2 & \epsilon & \dots & \\ & & & \vdots & \vdots & & \\ \dots & a_{jm} & \dots & \epsilon & 2 & \dots & \\ & & & \vdots & \vdots & & \end{pmatrix}.$$

The row and column operations  $R_j \rightarrow R_j \pm R_i$  and  $C_j \rightarrow C_j \pm C_i$ , where we use the plus sign if  $\epsilon = -1$  and the negative sign otherwise, give:

$$\begin{pmatrix} & & & \vdots & \vdots & & \\ & & & a_{mi} & x_{mj} & & \\ & & & \vdots & \vdots & & \\ \dots & a_{im} & \dots & 2 & -\epsilon & \dots & \\ & & & \vdots & \vdots & & \\ \dots & x_{jm} & \dots & -\epsilon & 2 & \dots & \\ & & & \vdots & \vdots & & \end{pmatrix}.$$

Now, let  $a_{mi} \neq 0$  and  $a_{mj} \neq 0$ , meaning that  $v_i$  and  $v_j$  are both connected to  $v_m$  forming a 3-cycle and since every cycle in  $G$  is assumed to be positive, if  $\epsilon = 1$ , then  $a_{mi} = a_{mj} = \pm 1$  and if  $\epsilon = -1$ , then  $a_{mi} = -a_{mj}$ . Hence, after the row and column operation,  $x_{mj} = 0$  and  $v_j$  loses its connection with  $v_m$ . If  $a_{mi} \neq 0$  and  $a_{mj} = 0$ , then  $x_{mj} = a_{mi}$  for  $\epsilon = -1$  and  $x_{mj} = -a_{mi}$  for  $\epsilon = 1$ , meaning that  $v_i$  is now connected to  $v_m$ . If  $a_{mi} = 0$  and  $a_{mj} \neq 0$ , then  $x_{mj} = a_{mj}$ . Hence, the above matrix can be written as  $2I + A(G')$  for some signed graph  $G'$ , where  $G'$  is precisely the graph that results from performing the move on  $G_1$  in the mentioned vertex and edge. Moreover, if  $G_1$  has positive cycles, then the cycles of  $G'$ , if any, are also positive so if there is a sequence of moves changing  $G_1$  into  $G_2$ , we can find a sequence of elementary operations changing  $2I + A(G_1)$  into  $2I + A(G_2)$ .  $\square$

It is clear now, that Theorem 3.1 and Lemma 3.2 implies that a positive definite matrix of the form  $2I + A(G)$ , for some signed graph  $G$ , is congruent over  $\mathbb{Z}$  to a matrix  $2I + A(\Gamma)$  where  $\Gamma$  is one of the ADE diagrams.

**Definition 3.9.** A  $t$ -move on a vertex  $v$  and edge  $(v, w)$  where  $\deg_w \in \{1, 2, 3\}$  will be called a  $t'$ -move. We say that two signed graphs  $G_1$  and  $G_2$  are  $t'$ -equivalent if there exists a sequence of  $t'$ -moves changing  $G_1$  into  $G_2$ . We denote it by  $G_1 \sim_{t'} G_2$ .

For instance, all the moves in Figures 3.3 to 3.5 are  $t'$ -moves. For the case of positive, planar graphs that admit a checkerboard coloring the  $t'$ -moves can be

restricted into the following three types (we have excluded the degree one case from Figure 3.6 for being trivial):

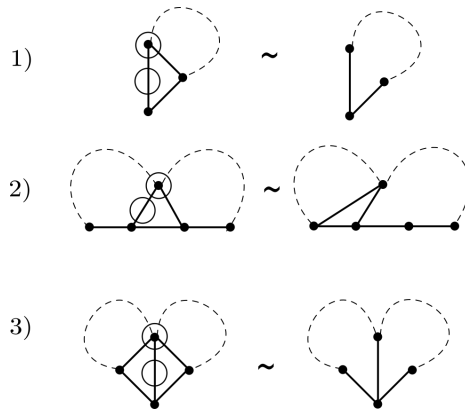


Figure 3.6: Dashed lines represents graphs connected to the line's endpoints.

To see that, note that positivity and checkerboard coloring properties on a planar signed graph  $G$  implies that the maximum degree of a vertex,  $v$ , in  $G$  is 6. Moreover,  $v$  is never an internal vertex (use Remark 3.6 and the fact that the wheel graph,  $W_7$ , is not positive). Also, exclude all the combinations that are  $t'$ -equivalent to a non-checkerborad graph, see for instance Figure 3.7 (such moves will not be allowed).

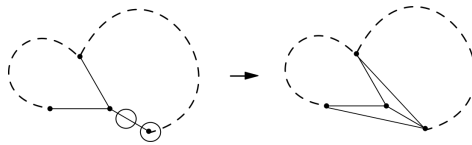


Figure 3.7

### 3.3 Proof of Theorems 3.1 and 3.2

In this section we first give the proof of Theorem 3.1. As explained in the introduction, the proof is done by induction. We assume that a graph,  $\Gamma$ , is  $t$ -equivalent to one of the  $ADE$  diagrams, so it is clear that if we add a vertex  $v$  to  $\Gamma$ , then  $\Gamma \cup v \sim ADE \cup v$ . Therefore, all we need to prove the Theorem 3.1 is to show that connecting a vertex to one of the  $ADE$  diagrams results, after a sequence of  $t'$ -moves, into another  $ADE$  diagram or a non-positive graph. We divide the proof in two parts: first, we study the case in which we add a vertex to the graph  $A_n$  and second, we study in a similar manner those in which we add a vertex to  $D_n$ ,  $E_6$ ,  $E_7$  and  $E_8$ . Finally, we prove Theorem 3.2.

**Proposition 3.10.** *If  $G_n$  is a positive signed graph with  $n$  vertices such that it is the union of  $A_{n-1}$  with an extra vertex connected to  $A_{n-1}$  by  $m$  edges, then  $G_n$  is  $t'$ -equivalent to one of the simply laced Dynkin diagrams.*

*Proof:* The graph  $|G_n|$  can be pictured as in Figure 3.8, where  $v_n$  has degree  $m$  and the number of cycles in  $G_n$  is therefore  $m - 1$ .

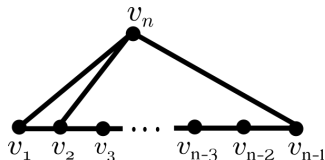


Figure 3.8: An example of  $|G_n|$  for  $m = 3$ .

Notice that, if  $m > 6$ , then we can easily find an induced subgraph of type  $X$  (see Figure 3.1) in  $G_n$ , implying that  $G_n$  is not positive. Therefore, in order to prove the proposition, we consider all possible graphs for  $m \leq 6$ , which we divide in the following cases, and show that each of them is either  $t'$ -equivalent to a graph that contains a forbidden minor or it is  $t'$ -equivalent to one of the graphs  $A_n$ ,  $D_n$ ,  $E_6$ ,  $E_7$  or  $E_8$ .

First, observe that if  $m = 6$ , then  $G_n$  contains five cycles and these must have length 3, otherwise  $G_n$  contains a minor of type  $X$ . Hence, if we perform a  $t'$ -move on  $v_n$  and the second and fifth edges we can reduce the degree of  $v_n$  by four, which brings us to the  $m = 2$  case. In a similar fashion, if  $m = 5$ , then there are four cycles in  $G_n$ . If at least two of these cycles have length  $> 3$ , then  $X \subset G_n$ . So there must be at least three cycles of length 3; one can easily check that after a  $t'$ -move on  $v_n$  and one of the edges shared by these 3-cycles,  $\deg_{v_n} = 3$ . Consequently, we just need to consider the following four cases, in which  $m$  takes the values 1, 2, 3 and 4.

**Remark 3.11:** Suppose that  $v_n$  is connected to  $v_1$  and  $m > 1$ , i.e.,  $v_n$  is connected to at least one other vertex, say  $v_x$ . If  $x = 2$ , then  $[v_n, v_1]$  reduces the degree of  $v_n$  by one. If  $x \neq 2$ , then  $[v_n, v_1]$  creates a 3-cycle and we can follow the sequence in Figure 3.4 in order to reduce the degree of  $v_n$  by one, the same argument works in the case that  $v_n$  is connected to  $v_{n-1}$ . Therefore, for the cases where  $m > 1$  we will assume that  $v_n$  is not connected to any of these.

*Case 1:* If  $m = 1$ , and  $v_n$  is connected to the vertex  $v_1$  (or  $v_{n-1}$ ), then  $G_n \sim_{t'} A_n$ . If  $v_n$  is connected to the vertex  $v_2$  (or  $v_{n-2}$ ), then  $G_n \sim_{t'} D_n$ . If  $v_n$  is connected to the vertex  $v_3$  (or  $v_{n-3}$ ), then for  $n > 8$ ;  $E \subset G$ , and for  $n \in \{6, 7, 8\}$ ;  $G \sim_{t'} E_n$ . If  $v_n$  is connected to a vertex different from those mentioned above and  $n \geq 8$ , then  $T \subset G$ .

*Case 2:* If  $m = 2$ , then there is one cycle in  $G_n$ , whose length we denote by  $x$ .

If  $x = 3$ , then  $G_n \sim_{t'} A_n$ , see Figure 3.3. If  $x = 4$ , then we obtain  $D_n$  by a  $t'$ -move on  $v_n$  and the two edges that have  $v_n$  as an endpoint leading to a graph of type  $B$  or (a). For  $x = 5$  we need to consider the following case:

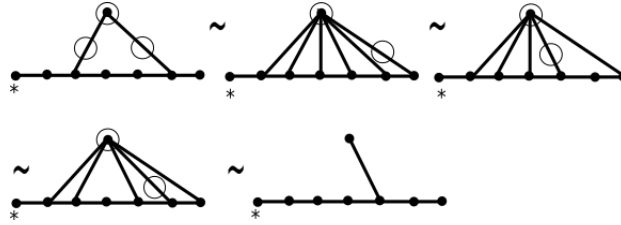


Figure 3.9: The non-signed graph without the starred vertex is  $t'$ -equivalent to  $E_7$ . The same  $t'$ -moves can be used with the additional starred vertex: leading to  $E_8$ .

From the graph in Figure 3.10, it is clear that if we connect a new vertex to the starred one the resulting graph is  $t'$ -equivalent to  $E$ . If instead we connect a new vertex as it appears in Figure 8, then  $G$  is  $t'$ -equivalent to a graph with a  $T$  minor.

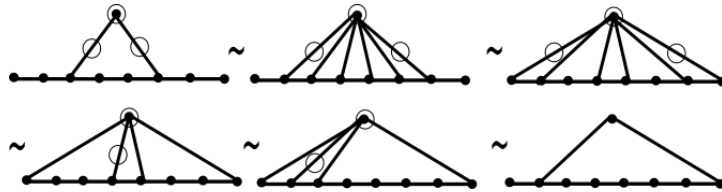


Figure 3.10: The non-signed graph is  $t'$ -equivalent to a graph that contains a  $T$  minor.

If  $x > 5$ , then  $G_n$  clearly contains a minor of type  $\tilde{D}$ .

*Case 3:* For  $m = 3$ , there are two cycles in  $G_n$ . If both of them have length 3, we can perform a  $t'$ -move as in Figure 3.4 (middle case) which boils down to the  $m = 1$  case. If there is only one cycle of length 3, then  $G_n$  is a  $B$  type graph and again, we are in case 1. If both cycles are  $\geq 4$ , then  $\tilde{D} \subset G_n$ .

*Case 4:* Now, consider  $m = 4$ , we know that there are three cycles in  $G_n$  and if they all have length  $> 3$ , then  $X \subset G_n$ . If there are two cycles with length  $> 3$  and the third has length 3, then we can reduce  $m$  by two as it is shown in Figure 3.11. There are two cases to consider:

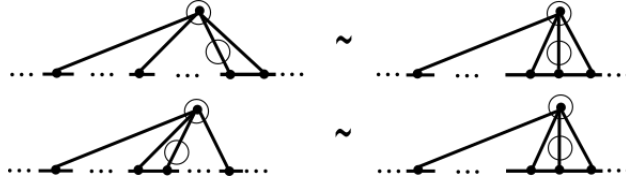


Figure 3.11

If there are two non-adjacent cycles of length 3 and one with length  $> 3$ , then  $G_n$  appears as in Figure 3.5(A), so  $G_n \sim_{t'} D_n$ . If there are two adjacent 3-cycles and one with length  $> 3$ , then we can reduce  $m$  by two, see Figure 3.11, and if all three cycles have length 3, then we can easily reduce  $m$  by two, see the diagram of Figure 3.5(A).  $\square$

*Proof of Theorem 3.1:* Let  $n$  be the number of vertices of  $G$ . We may assume  $n \geq 1$  and proceed by induction on  $n$ . For  $n = 1$  it is clear. Assume that the positive signed graph  $G_{n-1}$  with  $n - 1$  number of vertices is  $t'$ -equivalent to one of the  $ADE$  diagrams. In the following cases we show that if we connect one vertex to  $G_{n-1}$ , the new graph  $G$  is either  $t'$ -equivalent to one of the  $ADE$  diagrams or it is not positive (recall that we already know that this works for  $G_{n-1} \sim_{t'} A_{n-1}$ ). Note that in a connected graph  $G$  we can choose a vertex  $v$  such that  $G - v$  is connected (such a vertex exists; see e.g. [17]).

*Case 1:* Let  $G_{n-1} \sim D_{n-1}$  for  $n > 4$ , so the graph  $|G|$  can be pictured as in Figure 3.12, where  $v$  has degree  $m$ .

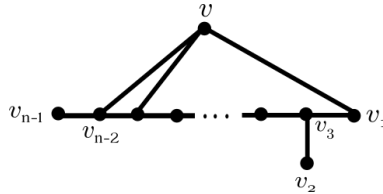


Figure 3.12: An example of  $|G|$  for  $m = 2$ .

If  $m > 6$ , then clearly  $X \subset G$ . Now recall that in the proof of Proposition 3.1 we only needed to consider the cases where  $m \in \{1, 2, 3, 4\}$ , similar arguments work for this case. In addition, we observe that if  $m > 2$  and  $v$  is connected to  $v_1$  and  $v_2$ , then there are two cycles sharing two edges, which makes  $G$  a non-positive graph for any choice of signs, see Remark 3.5. If that is not the case, then one can easily check that  $m$  can be reduced to 1, 2 or 3. Notice that, if  $v$  is not connected to  $v_1$ ,  $v_2$  and  $m > 1$ , then clearly  $\tilde{D} \subset G$  or  $X \subset G$  (except for  $m = 2$  and with a cycle of length 3, in which case  $G \sim_{t'} D_n$  by a  $t'$ -move). Thus, for  $m > 1$ , we will only consider the cases when  $v$  is connected to at least one of the vertices  $v_1$  and  $v_2$ .



*Case 1.1:* If  $m = 1$  and  $v$  is connected to the vertex  $v_1$  or  $v_2$  and  $n \leq 8$ , then  $G \sim_{t'} E_n$  for  $n \in \{6, 7, 8\}$ . If  $n > 8$ , then  $G$  contains an induced subgraph of type  $E$ . If  $v$  is connected to the vertex  $v_{n-1}$ , then  $G_{n+1} \sim_{t'} D_{n+1}$ . If  $v$  is connected to any other vertices, then  $\tilde{D} \subset G$  or  $X \subset G$ .

*Case 1.2:* If  $m = 2$ , the cycle has length 3 and  $v$  is connected to  $v_1$  (or  $v_2$ ) and  $v_3$ , then  $G \sim_{t'} E_n$  for  $n \in \{6, 7, 8\}$  by a  $t'$ -move on  $[v, v_1]$  (or  $[v, v_2]$ ), and it contains an  $E$  minor for  $n > 8$ . If the cycle has length  $> 3$  and  $v$  is connected to  $v_i$  and  $v_j$  for  $j = n - 1$  and  $i \in \{1, 2\}$ , then  $G$  can be treated as one of the graphs in the proof of Proposition 3.10. But, if  $3 < j < n - 1$  and  $i \in \{1, 2\}$ , then one can check that:



Figure 3.13

This again brings us to Proposition 3.10. Finally, if  $v$  is connected to  $v_1$  and  $v_2$ , then  $G$  can also be treated as one of the graphs in the proof of Proposition 3.10.

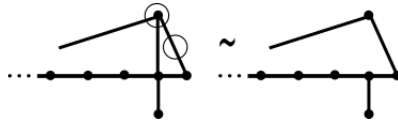
*Case 1.3:* If  $m = 3$ , then  $G$  has two cycles:

- If both cycles have length 3 and  $v$  is connected to  $v_1, v_2$  and  $v_3$ , then

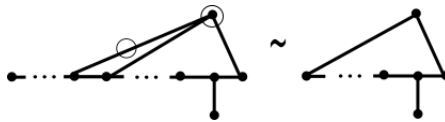


Figure 3.14: The non-signed graph is  $t'$ -equivalent to a graph as in the proof of Proposition 3.10, case 2.

- If there is only one cycle with length 3, we need to consider either the case:



or



both of them reduce to case 1.2.

- If both cycles have length  $> 3$ , then we need to consider the following cases:
  - $v$  is connected to  $v_1, v_2$  and  $v_i$  for  $3 \leq i \leq n-1$ , then  $G$  has two cycles sharing two edges so by Remark 3.5,  $G$  is not positive.
  - $v$  is connected to  $v_1, v_{n-1}$  and  $v_i$  for  $3 < i < n-1$ , then  $G$  is as in Figure 3.13 (middle case).
  - If  $v$  is connected to  $v_1$  and two other vertices different from  $v_{n-1}, v_2$  and  $v_3$ , then the only relevant case is when both cycles have length 4 since for any other lengths one can easily find a minor of type  $\tilde{D}$  or  $X$ . In the former case, Figure 3.15 shows that we can reduce it to case 1.2.

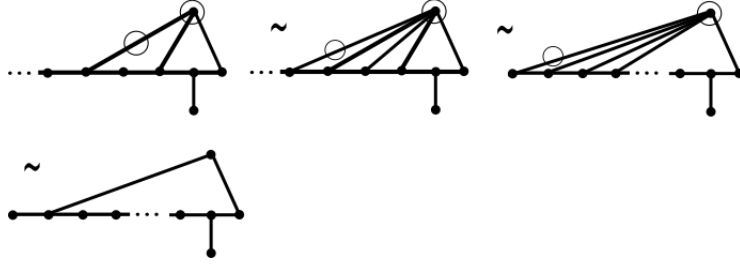


Figure 3.15

*Case 2:* Assume  $G_{n-1}$  is  $t'$ -equivalent to  $E_6, E_7$  or  $E_8$ . So we can picture the graph  $|G|$  as in Figure 3.16.

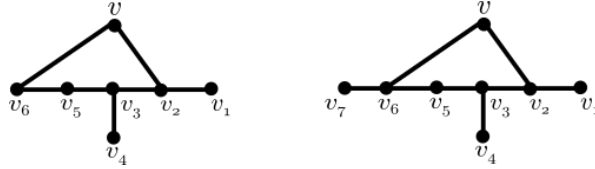


Figure 3.16: Examples of  $|G|$  for  $m = 2$ . Left:  $G_{n-1} \sim_{t'} E_6$ . Right:  $G_{n-1} \sim_{t'} E_7$ . We can construct the  $E_8$  case by simply connecting a new vertex, say  $v_8$ , to  $v_7$ .

*Case 2.1:* First, consider that  $G_{n-1} \sim_{t'} E_6$ . If  $m = 1$  and  $v$  is connected to the vertex  $v_1$  or  $v_6$ , then  $G \sim_{t'} E_7$ . If  $v$  is connected to the vertex  $v_3$ , then  $X \subset G$ . If  $v$  is connected to a vertex different from those mentioned above, then  $G$  contains an induced subgraph of type  $\tilde{D}$ . The case where  $G_{n-1} \sim_{t'} E_7$  works similarly, and if  $\sim_{t'} E_8$ , then either we encounter the induced subgraphs  $\tilde{D}, T$  and  $X$ , or  $G = E$ .

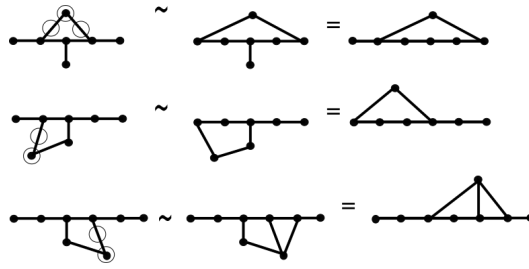


Figure 3.17

$G_{n-1}$	$E_6$	$E_7$	$E_8$	$E_6$	$E_7$	$E_8$
4						
5						
6						
7						
8						

Figure 3.18: The graphs encircled with green contain an induced subgraph of type  $X$ , those encircled in blue contain  $\tilde{D}$ , and those in red contain  $Y$ . The right column includes the graphs in which  $v$  is connected to  $v_4$ . The graphs that are not encircled are  $t'$ -equivalent to  $E_7$ ,  $E_8$  or, in the case where  $G_{n-1} \sim_{t'} E_8$ , to a graph with the induced subgraph  $E$ .

*Case 2.2:* Let  $m = 2$  so  $G$  has one cycle of length  $x$ . First, if  $x = 3$  and  $v$  is connected to  $v_3$  and  $v_4$ , then  $G \sim_{t'} Y$  (by a  $t'$ -move on  $[v, v_4]$ ). If  $G_{n-1} \sim_{t'} E_6$  and  $v$  is connected to a different pair of vertices, then  $G \sim_{t'} E_7$ ; however, that is not the case for  $G_{n-1} \sim_{t'} E_7$ , in which we can still find it is  $t'$ -equivalent to  $E_8$  or it contains  $T$ . If  $G_{n-1} \sim_{t'} E_8$ , then it does not matter to which vertices we connect  $v$ , the resulting graph is  $t$ -equivalent to a graph with  $T$  or  $E$  as a minor. Now, for the cases where  $x > 3$  we simply draw all possible diagrams, see Figure 3.18, and we find that they are either non-positive or  $t'$ -equivalent to  $E_7$  or  $E_8$  (see Figure 3.17).

*Case 2.3:* If  $m = 3$  and both cycles have length 3, we can easily reduce the degree of  $m$  by a  $t'$ -move, bringing us to the cases 2.1 or to the case 2.2 if  $v$  is connected to  $v_3$ . If there is only one cycle of length 3, then we can reduce the degree by one. If both cycles have length  $> 3$ , one can check all possibilities as we did in Figure 3.18, and find that all of them contain either  $X$  or  $\tilde{D}$ .

Finally, if  $m > 3$  we can easily reduce the degree of  $v$  by using  $t'$ -moves; taking us to the previous cases.  $\square$

**Lemma 3.12.** *Let  $G$  be a positive signed checkerboard graph with  $n \geq 3$  vertices, then there exists at least one vertex in  $G$  of degree 2 or 3.*

*Proof:* We show that if  $G$  is a graph whose vertices have degree one or  $\geq 4$ , then  $G$  is not positive. Recall from the previous section that positivity and checkerboard coloring properties on  $G$  implies that the maximum degree of a vertex,  $v$ , in  $G$  is 6 and  $v$  is never an internal vertex. Now, if  $v$  is a vertex in  $G$  of degree six, then the graphs on the first row in Figure 3.19 are the only two possible induced subgraphs involving  $v$  in  $G$  (any other combination is a non-positive graph). Similarly, if the degree of  $v$  is five or four, we find that the graphs on the second and third row of Figure 3.19 are the possible induced subgraphs involving  $v$ .

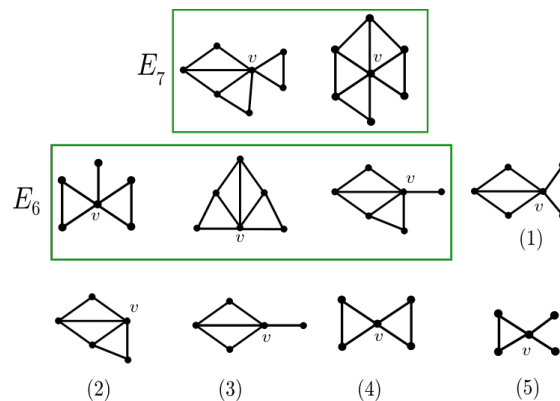


Figure 3.19

Theorem 3.1 shows that connecting a vertex to one of the special Dynkin graphs results into a graph in this class or into a non-positive one. Since the graphs in the green boxes of Figure 3.19 are  $t'$ -equivalent to  $E_6$  or  $E_7$ , connecting more than two vertices to them will result into a non-positive graph. Thus, if we want to construct a positive graph whose vertices have degree one or  $\geq 4$ , we cannot use the graphs inside the boxes.

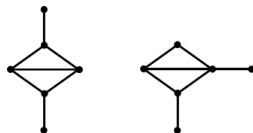


Figure 3.20: Two graphs  $t'$ -equivalent to  $E_6$ .

Now, consider the graphs in Figure 3.20, they are  $t'$ -equivalent to  $E_6$ . It is not hard to see that we cannot increase to 4 the degree of all the adjacent vertices of  $v$  in the graph (3), Figure 3.19 without encountering one of the graphs in Figure 3.20 (neither in (1), since  $(3) \subset (1)$ ). Indeed, for the graphs (2), (4) and (5) only connecting triangles as it appears in Figure 3.21 will work, but since the graph must have all its vertices of degree  $\geq 4$  or one, for every vertex in the triangles we need to add at least two more vertices of degree one, creating a  $\tilde{D}$  minor. Note that, joining two vertices of different triangles by an edge in the first graph of Figure 3.21 results into a non-positive graph by Remark 3.6. By the same reason, we cannot join more than two triangles in the second graph. As for the fourth one, joining them results into a non-positive graph by direct computation.

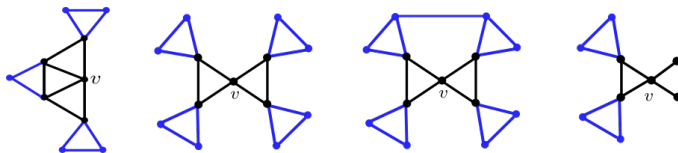


Figure 3.21

□

**Lemma 3.13.** *Let  $\Gamma$  be a positive signed checkerboard graph. If there is a sequence of moves such that  $\Gamma$  is  $t'$ -equivalent to one of the ADE diagrams, then  $\Gamma \cup v$  is  $t'$ -equivalent to one of the ADE diagrams union  $v$ .*

*Proof:* If there is a sequence of moves such that  $\Gamma$  is  $t'$ -equivalent to one of the ADE diagrams and if  $\Gamma \cup v$  is such that all the vertices in  $\Gamma$  connected to  $v$  have degree 2 or 3, then the same sequence can be used to transform  $\Gamma \cup v$  into one of the ADE diagrams union  $v$ . If the degree of a vertex connected to  $v$  is  $\geq 4$ , then we cannot always use the same sequence. However, as we prove next, we

can always find a  $t'$ -sequence that transform  $\Gamma \cup v$  into one of the ADE diagrams union  $v$ .

Let  $G$  be a positive planar graph such that it has a finite set of vertices of degree  $\geq 4$ , then there is a  $t'$ -sequence that transforms  $G$  into a graph whose vertices have degree at most 3. In order to prove it, assume that there exists in  $G$  at least one vertex, say  $w$ , of degree  $\geq 4$  that cannot be reduced by  $t'$ -moves to a degree  $\leq 3$ . Using Figure 3.19, this means that at least three adjacent vertices of  $w$  must have degree  $\geq 4$  and cannot be reduced to lower degrees ( $\leq 3$ ) either. By the proof of Lemma 3.12 we know that such graph is not positive.

Now, let us come back to the case where  $v$  is connected to a set of vertices of  $\Gamma$ , some of them with degree  $\geq 4$ . Then, we can find a sequence of  $t'$ -moves that transforms  $\Gamma \cup v$  into  $\Gamma' \cup v$  where  $\Gamma'$  is positive and all its vertices have degree  $\leq 3$ . Thus, by Theorem 3.1 there is a sequence of  $t$ -moves transforming  $\Gamma'$  into one of the ADE diagrams; but since all its vertices are of degree less or equal three, the statement follows.  $\square$

*Proof of Theorem 3.2:* We prove it by induction on the number of vertices. Assume that there is a sequence such that  $\Gamma$  is  $t'$ -equivalent to one of the ADE diagrams. By Lemma 3.13 we know that there is a  $t'$ -sequence transforming  $\Gamma \cup v$  into one of the ADE diagrams union  $v$ , denote this graph by  $G$ . Now, analogous to the proof of Theorem 3.1 we get that  $G$  is  $t'$ -equivalent to one of the ADE diagrams, completing the proof.  $\square$

### 3.4 Moves on checkerboard graphs

In this section we show that we can associate a signed graph to a checkerboard graph. We provide two checkerboard graph moves that preserve the corresponding link type; these are nothing but a generalization of the moves in [2]. Finally, we use these facts together with Theorem 3.2 to prove Theorem 3.3.

Recall from the definition of a checkerboard graph  $\Gamma$ , as it appears in [3], that this defines a strongly quasipositive fibred link,  $L(\Gamma)$ , constructed by plumbing positive Hopf bands according to the graph  $\Gamma$ . The signature,  $\sigma(L(\Gamma))$ , as defined by Trotter [34], is the signature of the symmetric matrix  $M = V + V^T$ . Thus, if  $L(\Gamma)$  has maximal signature,  $M$  must be a positive definite matrix. It follows that  $M = [x_{ij}]$  is a symmetric matrix such that  $x_{ij} = 2$  if  $i = j$ . Now, since  $x^T M x > 0$  for every non-zero vector  $x \in \mathbb{R}^n$ , choose  $x = e_i \pm e_j$  then  $(e_i + e_j)^T M (e_i + e_j) = 2x_{ij} + 4 > 0$  for all  $1 < i, j < n$  and  $(e_i - e_j)^T M (e_i - e_j) = -2x_{ij} + 4 > 0$ . Therefore,  $|x_{ij}| < 2$  if  $i \neq j$ , and the non-diagonal coefficients are 0, 1 or  $-1$ . So  $M$  is one of a finite list of matrices, and these can be represented by signed graphs. Moreover, since the vertices in a checkerboard graph and the ones in the corresponding signed graph represents positive Hopf bands, and two vertices are connected whenever the core

curves of the corresponding Hopf bands intersect, it follows that the underlying graph of a checkerboard graph and the one of the corresponding signed graph are the same.

**Lemma 3.14.** *The following two checkerboard graph moves preserve the corresponding link types.*

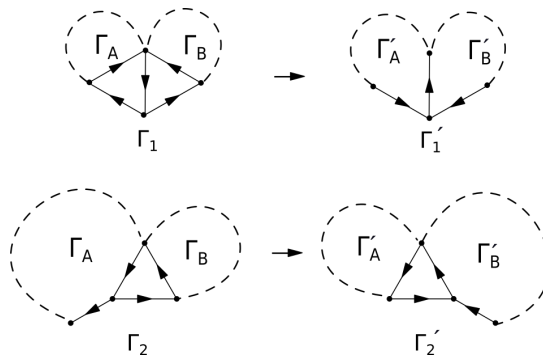


Figure 3.22:  $\Gamma_A$  and  $\Gamma_B$  represents checkerboard graphs connected to the dashed line's endpoints.

*Proof:* Recall that we can associate an abstract open book to a checkerboard graph. The goal is to show that the open books associated to the graphs  $\Gamma_1$  and  $\Gamma'_1$  are equivalent, i.e. let  $(\Sigma_1, \phi_1)$  and  $(\Sigma'_1, \phi'_1)$  be the open books associated to the graphs, then there is a diffeomorphism,  $h$ , between the surfaces  $\Sigma_1$  and  $\Sigma'_1$  such that  $h \circ \phi'_1 = \phi_1 \circ h$ . To do so, we will use the same argument as in [2] and check that these surfaces, equipped with a family of preferred curves, differ by a Dehn twist.

The way we construct an abstract open book from a checkerboard graph is by gluing annuli; one for each vertex in  $\Gamma$ , and gluing disks; one for each cycle. The orientation of the core curves in each annulus is chosen so the intersection numbers with the other core curves corresponds to the orientations of the edges in  $\Gamma$ , see [3] for further details about the construction. We can now construct the surface associated with  $\Gamma_1$ , see Figure 3.23 (left), where the grey areas represents the disks and in the yellow squares we glue the parts that correspond to  $\Gamma_A$  and  $\Gamma_B$ . Recall that the monodromy,  $\phi$ , is the product of positive Dehn twists in a certain order indicated by the orientation of the edges in  $\Gamma_1$ . In our case, if we label the vertices by  $\alpha, \beta, \gamma, \delta$ , one for each core curve in the surface and we take into account the orientation of the cycles  $A$  and  $B$ , the monodromy can be written as  $\phi_A \phi_B T_\gamma T_\delta T_\alpha T_\beta$  (it is customary to write  $T_a$  as the Dehn twist of the curve  $a$ ), where we have used the fact that we can switch two elements if there is no edge between them [3].

After performing a Dehn twist on  $\delta$  along  $\alpha$  we obtain the surface on the right, which one can easily check that corresponds to  $\Gamma'_1$ . Since  $\delta' = T_\alpha^{-1}(\delta)$ , then

$T_{\delta'} = T_{\alpha}^{-1}T_{\delta}T_{\alpha}$  and  $T_{\alpha}T_{\delta'} = T_{\delta}T_{\alpha}$ . The monodromy is isotopic to  $\phi_A\phi_B T_{\gamma}T_{\alpha}T_{\delta'}T_{\beta}$  which is precisely the monodromy that we obtain from the surface in the right.

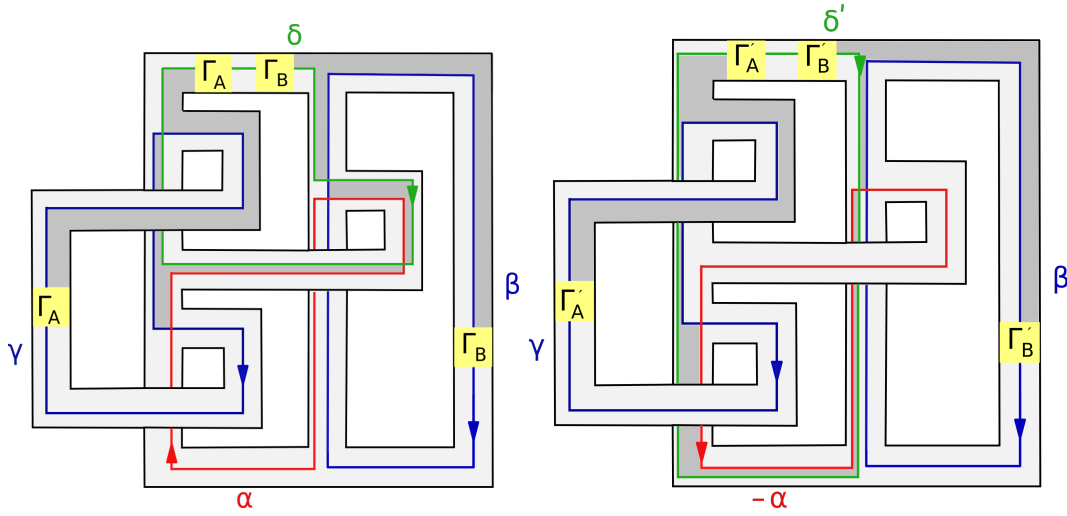


Figure 3.23: This drawing is a modification of a drawing in [2]. Right: four positive Hopf bands plumbed according to the graph in Figure 3.22 with four 2-handles(shaded regions). Left: the surface after a Dehn twist of  $\delta$  along  $\alpha$ .

The second move is a generalization of the one described in [2], only that this time we have the cycles  $A$  and  $B$ , forming new grey regions as indicated in the corresponding abstract surfaces in Figure 3.24. It is easy to check that the proof also works in this case.  $\square$

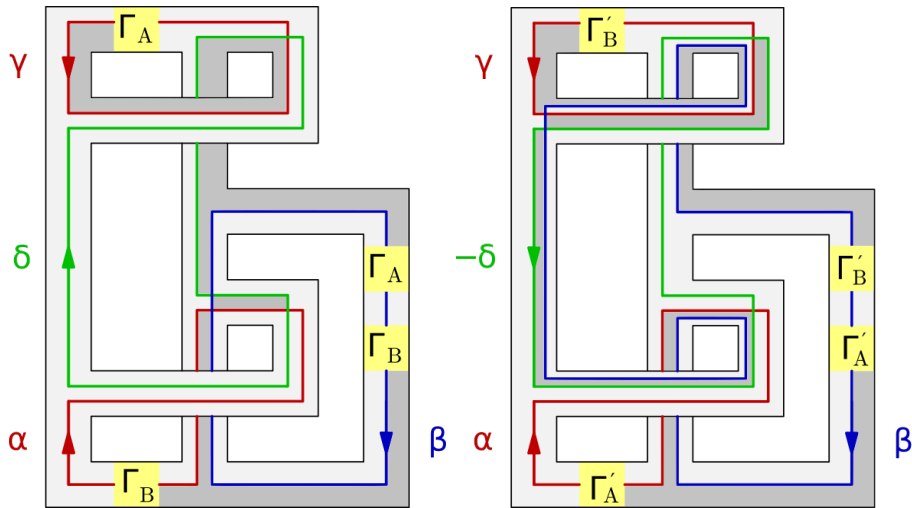


Figure 3.24: Right: four positive Hopf bands plumbed according to the graph in Figure 3.22 with three 2-handles(shaded regions). Left: the surface after a Dehn twist of  $\beta$  along  $\delta$ .

*Proof of Theorem 3.3:* Let  $\Gamma$  be a checkerboard graph and let  $L(\Gamma)$  be the



associated link with maximal signature. We know that we can associate a signed graph, say  $\Gamma^\pm$ , to  $\Gamma$  and by Theorem 3.2. there exists a sequence of  $t'$ -moves that transforms  $\Gamma^\pm$  into one of the *ADE* diagrams. Therefore, we can find a sequence of the moves in Lemma 4.14. (note that the moves in Figure 3.22 are a checkerboard graph version of the  $t'$ -moves in Figure 3.6) that transforms  $\Gamma$  into a checkerboard graph of *ADE* type preserving the corresponding link type.  $\square$



## Chapter 4

# Balloon graphs

In this chapter we characterize the checkerboard graphs whose corresponding links are isotopic to the ones realized by the simply laced Dynkin diagram  $D_n$ ,  $A_n$ ,  $E_6$  and  $E_7$ . Finally, we use these results to prove that there exists a linear time algorithm for finding definite checkerboard graphs.

### 4.1 Introduction

In the previous chapter we showed that checkerboard graph links with maximal signature are isotopic to one of the ADE links. Here, we answer the question of how these checkerboard graphs look like. The motivation behind is to determine if there exists a linear time algorithm to detect links with maximal signature out of a checkerboard graph. In [2] it is shown that it is possible to characterize linking graphs whose corresponding links are isotopic to  $L(A_n)$ , such graphs were named by *triangle tree graphs*, we define this in the next section. Consequently, they found the existence of a linear time algorithm to detect  $L(A_n)$  out of a linking graph.

The *line graph* of a graph, is one in which every vertex represents an edge, and two vertices are adjacent if and only if their corresponding edges share a vertex. Graphs with eigenvalues greater than  $-2$  have been characterized in [13], Theorem 2.1 showing that such graphs are either one of a finite list of graphs (corresponding to the  $E_{6,7,8}$ ), the line graph of a tree or an odd unicycle graph, or a certain *generalized line graph*, we refer the reader to [9] for a definition of the latter graphs. A similar result was found in [19] for the case of signed graphs. It is worth mentioning that the triangle tree graphs can be defined as the line graph of a tree. In fact, one could recover the graphs introduced in Proposition 4.1 using the definitions in [19] and [13]. Here, we rediscover these graphs in the context of checkerboard graph links.

**Proposition 4.1.** *Let  $\Gamma$  be a checkerboard graph with  $n$  vertices and  $L(\Gamma)$  the associated link. Then,  $L(\Gamma)$  is isotopic to  $L(D_n)$  if and only if  $\Gamma$  is either a 1-balloon graph or one of the three types of graphs in Figure 4.1 below, where the dashed circles represent triangle tree graphs.*

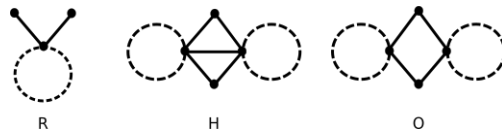


Figure 4.1: The underlying graphs of type  $R$ ,  $H$  and  $O$ . The triangle tree graph in  $R$  must contain at least one edge.

The triangle tree and 1-balloon graphs will be defined in the following section. To show that checkerboard graph links of the four types above are isotopic to  $L(D_n)$  is rather easy if we consider the  $t'$ -moves. Although originally the move carries a change of orientation in the graph we will consider only graph moves on the unoriented level as we did in the previous chapter.

We speak of the equivalence class of a graph as the set of all graphs that arise from it by using sequences of  $t'$ -moves. For the second part of the proof, we use two main ingredients: one is a list of criteria to determine when the graph is not positive, like for example the list of forbidden minors  $E$ ,  $X$ ,  $Y$ ,  $T$  and  $\tilde{D}$ , see Figure 3.1, and the second is to treat the equivalence class of  $E_6$  as forbidden minors. Recall that in [2] they use the equivalence class of  $D_4$  as forbidden minors for the characterization of triangle tree graphs, which consist of a bicycle (an  $H$  graph without the triangle tree graphs attached to it) and a big cycle, i.e. a cycle with more than 3 vertices.

## 4.2 Balloon graphs

In this section we define  $m$ -balloon graphs and we show that they are  $t'$ -equivalent to  $D_n$  for  $m = 1$ . A straightforward definition of  $m$ -balloon graphs is that they are the line graphs of a planar graph with exactly  $m$  non-adjacent big cycles. Here, we say that two cycles are adjacent when they share at least one edge. However, it will be useful to have a better understanding of their structure in order to prove that they are  $t'$ -equivalent to  $D_n$ , that is why we will give the following more detailed definitions. Recall from [2] that a triangle tree graph can be constructed from a forest of maximal degree 3, by substituting every vertex of degree three with a triangle. It is easy to show that a triangle tree graph is  $t'$ -equivalent to  $A_n$ .

**Definition 4.2.** A balloon graph is a finite and planar  $n$ -cycle for  $n > 2$  with an arbitrary number (from 0 to  $n$ ) of triangles glued to its edges and such that these triangles are not adjacent between each other. That leaves one vertex for each triangle that does not belong to the  $n$ -cycle, we call these the free vertices of a balloon graph.

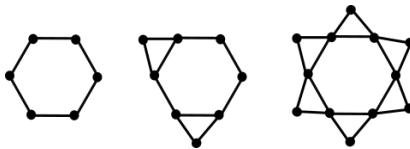


Figure 4.2: Three examples of balloon graphs with 0, 2 and 6 triangles (glued to its edges).

In a *triangle graph*, the vertices of degree 2 that belong to a cycle and the 1-degree vertices will receive the name of *free vertices* of a triangle graph. It is clear that every triangle graph has at least one free vertex. Similarly, for the graphs R, H and O, we will define as the free vertices the ones that connect to the triangle tree graph, see Figure 4.1.

**Definition 4.3.** Consider  $m \geq 1$  balloon graphs, each of them having at least one free vertex and  $x \geq 0$  triangle tree graphs (for the case where  $m = 1$  and  $x = 0$ , the balloon graph is not required to have free vertices). With these two ingredients we can construct a finite, connected graph by identifying free vertices in such a way that the dual of the resulting graph, without the vertex corresponding to the unbounded face, is a forest. Such graphs will receive the name of  $m$ -balloon graphs.

It is clear from the definition that a  $m$ -balloon graph admits a checkerboard coloring.

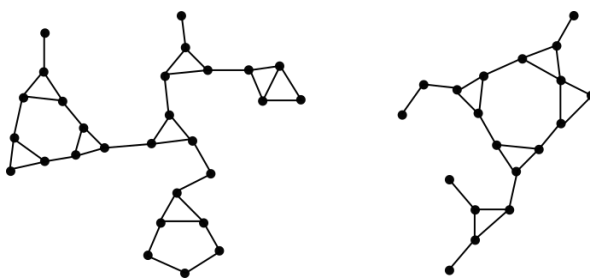


Figure 4.3: An example of a 3-balloon graph (left), and a 1-balloon graph (right).

**Remark 4.4.** The simplest 1-balloon graph is an  $n$ -cycle without free vertices, and we know from the previous chapter that such a graph is  $t'$ -equivalent to  $D_n$ .

Now, consider a 1-balloon graph,  $G$ , with  $n > 2$  vertices and assume that at least one of them is a free vertex. If it has no triangle graphs connected to it, applying step 3 in Figure 4.4 for each of its triangles will transform  $G$  into an  $n$ -cycle. If  $G$  contains triangle graphs, we can proceed as in Figure 4.4 for each triangle, transforming  $G$  into a  $n$ -cycle. Thus, it follows that a 1-balloon graph is  $t'$ -equivalent to  $D_n$ .

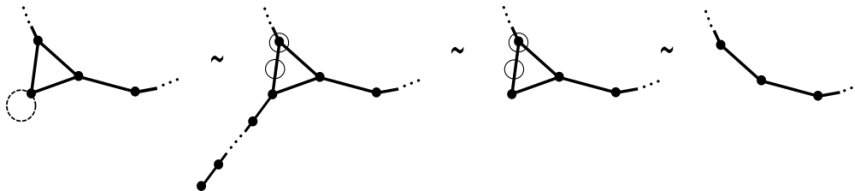


Figure 4.4: The dashed circle represents a triangle graph and the small circles mark the vertex and edge chosen for the  $t'$ -move.

An important observation is that an  $m$ -balloon graph is not positive for  $m > 1$ . In particular, it appears that 2-balloon graphs are  $t'$ -equivalent to  $\tilde{D}$ .

### 4.3 Proof of Proposition 4.1

**Lemma 4.5.** *Let  $G$  be a checkerboard graph  $t'$ -equivalent to  $D_n$ , then:*

- (i)  $G$  has none of the equivalence classes of  $E_6$ ,  $E$ ,  $X$ ,  $T$ ,  $Y$  and  $\tilde{D}$  as induced subgraphs.
- (ii)  $G$  has no internal vertices and the maximal degree of a vertex is 4.
- (iii)  $G$  does not contain any combination of at least two of the graphs  $R$ ,  $H$ , 1-balloon or  $O$  connected by their free vertices.

*Proof:* (i) It is clear that the minors  $E$ ,  $X$ ,  $T$ ,  $Y$  and  $\tilde{D}$  form a non-positive graph, [1]. Also, Theorem 3.3, shows that connecting a vertex to one of the special Dynkin diagrams ( $E_6$ ,  $E_7$  and  $E_8$ ) results into a graph in this class or into a non-positive one. Therefore, if  $G \sim D_n$ , then  $E_6$  is not an induced subgraph of  $G$ . For (ii) see the proof of Lemma 3.12. (iii) Observe that if  $G$  contains any combination of at least two of the graphs  $R$ ,  $H$  or  $O$  connected by their free vertices, we get  $\tilde{D}$  or  $X$  as an induced subgraph of  $G$ . Also, since a 1-balloon graph is  $t'$ -equivalent to  $D_n$ , it follows that any combination of the latter graphs with a 1-balloon is also  $t'$ -equivalent to a graph with  $\tilde{D}$  as an induced subgraph, see for instance the graphs in Figure 4.5.

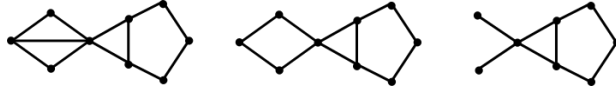


Figure 4.5: From left to right: H+1-balloon, O+1-balloon, R+1-balloon.

□

*Proof of Proposition 4.1:* We begin by proving that if  $G$  is  $t'$ -equivalent to  $D_n$ , then  $G$  must be one of the graphs  $R$ ,  $H$ ,  $O$  or a 1-balloon.

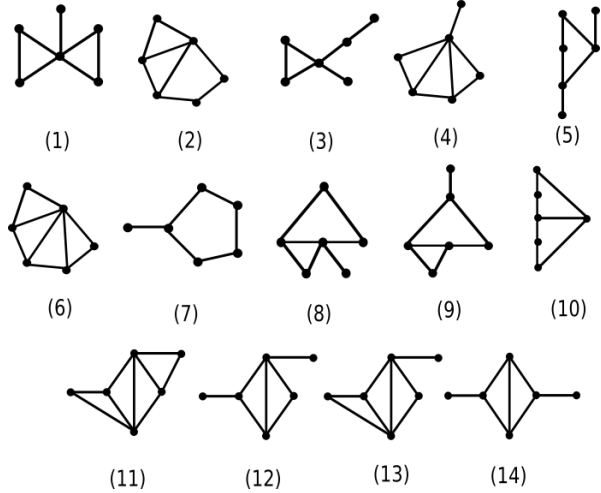


Figure 4.6: Complete list of checkerboard graphs  $t'$ -equivalent to  $E_6$ . Note that all of them qualify as linking graphs.

Let us start by assuming that  $G$  is a tree graph. Because of the minor  $X$ , the maximum degree of a vertex in  $G$  is 3, and  $G$  can only have one vertex of such degree, otherwise  $\tilde{D}$  is an induced subgraph in  $G$ . Thus,  $G$  must be  $D_n$ . The next step is to analyze  $G$  when it contains cycles. For that, we consider the following three cases:

**Case 1** *If  $G$  has two adjacent cycles, then  $G$  is either a 1-balloon graph or an  $H$  graph.*

First, it follows from Lemma 4.5 (ii) that these two cycles must share exactly one edge, and since  $G$  admits a checkerboard coloring, there cannot be a third cycle adjacent with the previous two. So, if both cycles have length  $> 4$ , then  $\tilde{D}$  is an induced subgraph in  $G$ . In the case where the lengths of the cycles are 4 and  $x \geq 4$ ,  $G$  contains a graph  $t'$ -equivalent to  $E_6$ ,  $E_7$  and  $E_8$  if  $x = \{4, 5, 6\}$  (see Figure 4.7 and Figure 4.6, graph 10), and for  $x > 6$ ,

$G$  contains a graph  $t'$ -equivalent to  $E$ . Therefore, we are left with the cases where the cycles length are 3 and  $x \geq 3$ .

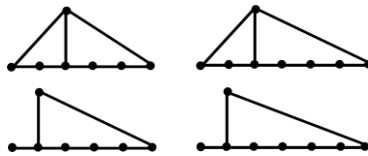


Figure 4.7: Top: two graphs  $t'$ -equivalent to  $E_7$  and  $E_8$  with cycle lengths  $(4, 5)$  and  $(4, 6)$ , respectively. Bottom: two graphs  $t'$ -equivalent to  $E_7$  and  $E_8$ .

First, consider the case where the cycles length are 3 and  $x > 3$  (this is nothing but a balloon with one triangle), we will use induction on the number of vertices that we add to it, in order to show that  $G$  is a 1-balloon graph. Let us start by connecting one vertex,  $v$ , of degree 1. A quick view shows that this is only possible if we connect it to the free vertex of the balloon, otherwise we get the minors (8) or (9) if  $x = 4$ , (7) if  $x = 5$  or the ones in Figure 4.7 for  $x \in \{6, 7\}$  and for  $x > 7$ , we get an  $T$  as an induced subgraph, see Figure 3.10. If the  $\deg_v = 2$  and we connect it to two adjacent vertices (forming a triangle), either we connect it by adding triangles to the balloon or the minors (2) for  $x = 4$  and (12) for  $x > 4$  appear. If we connect it to two non-adjacent edges then we encounter interior vertices. Now, given a balloon graph it is not hard to see that adding a vertex of degree  $\geq 3$  creates interior vertices.

Note that, from Proposition 3.10. adding a vertex to a triangle tree graph results into one of the simply laced Dynkin diagrams or a non-positive one, since the only outcome we are interested in, is when the resulting graph is  $t'$ -equivalent to  $A_n$  (otherwise  $G$  is not positive by Lemma 4.5 (iii)), we conclude that the new vertex together with the triangle tree graph must be another triangle tree graph. Therefore, the only way of connecting a vertex to a 1-balloon graph is by preserving the 1-balloon structure.

With a little more effort one can show that for the case where the cycles length are 3,  $G$  must be either a 1-balloon graph or an H graph.

**Case 2** *If  $G$  has two non-adjacent cycles sharing one vertex  $v$ , and there is not a third cycle adjacent with both of them, then either these two cycles have length 3 or  $G$  is an  $O$  graph. Moreover, in both cases  $\deg_v = 4$ .*

It is clear that if both cycles have lengths  $\geq 4$ , then  $X$  is an induced subgraph in  $G$ . If the cycles have lengths 3 and  $x > 4$ , then  $G$  contains the graph (7)



in Figure 4.6, one of the graphs in Figure 4.7 for  $6 \geq x \geq 7$  or a  $T$  minor for  $x > 7$ . If the cycles have lengths 3 and 4, then  $\deg_v = 4$ , otherwise  $X$  is an induced subgraph in  $G$ . Now, we can proceed by induction on the number of vertices that we add as we did in case 1, assuming that  $G$  is an  $O$  graph (see Figure 4.8, where the graphs A, B and C are triangle tree graphs) and connecting a vertex,  $v$ , results in the following three cases, depending on its degree.

- If  $\deg_v = 1$ , we cannot connect  $v$  to the vertices 2 and 3 because that would create an induced subgraph like the one in (5), neither to the vertex 1 (we get an  $X$  minor).
- If  $\deg_v = 2$ , connecting  $v$  by forming a triangle would create a graph of type (8), (9) or a  $H+O$ , 1-ball+ $O$  graph. If connected to non-adjacent vertices then either we get interior vertices, the minor (10) or, in the case we connect two triangle tree graphs we get a 1-ball+ $O$  graph.
- If we add a vertex of degree  $> 2$  we get either interior vertices or one of the minors in Figure 4.6.

Therefore, since the only way of connecting a vertex is in the triangle tree graphs A, B or C, we conclude that  $G$  must be an  $O$  graph.

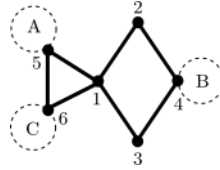


Figure 4.8

If both cycles have length 3, then  $\deg_v = 4$ , otherwise the graph in (1) would be an induced subgraph. Also, it follows immediately that there cannot be more than two non-adjacent cycles sharing a vertex.

**Case 3** *If  $G$  has a vertex  $v$ , belonging to exactly one cycle and  $\deg_v = 3$ , then either the cycle has length 3 or it has length 4 and  $G$  is an  $O$  graph. If  $\deg_v = 4$ , then the cycle must have length 3 and  $G$  is an  $R$  graph.*

First, if the degree of  $v$  is 3, then the cycle must have length 3 or 4 (for greater lengths we encounter the graphs in Figure 4.7 or Figure 4.6, (7)), for the latter case we can proceed similarly as we did in Case 2, proving that  $G$  must be an  $O$  graph. Second, if the degree of  $v$  is 4, then the cycle must have length 3 (otherwise  $X$  is an induced subgraph) and since the graph (3) is  $t'$ -equivalent to  $E_6$ , we conclude that  $G$  must be an  $R$  graph.

Now, since triangle-tree graphs are  $t'$ -equivalent to  $A_n$  it is straightforward that  $R \sim_{t'} D_n$ . The  $t'$ -move below shows that  $H \sim_{t'} O$  and by Proposition 3.10 we have that  $O \sim_{t'} D_n$ . Finally, recall that Remark 4.4 shows that a 1-balloon graph is  $t'$ -equivalent to  $D_n$ , which completes the proof.



Figure 4.9

□

## 4.4 Linear time algorithm

We will start by proving the following:

**Corollary 4.6:** *Let  $G$  be a checkerboard graph such that:*

- (i)  *$G$  has none of the equivalence classes of  $E_6$ ,  $E$ ,  $X$ ,  $T$ ,  $Y$  and  $\tilde{D}$  as induced subgraphs.*
- (ii)  *$G$  has no internal vertices and the maximal degree of a vertex is 4.*
- (iii)  *$G$  does not contain any combination of at least two of the graphs  $R$ ,  $H$ , 1-balloon or  $O$  connected by their free vertices.*

*Then,  $G$  is  $t'$ -equivalent to  $D_n$  or  $A_n$ .*

*Proof:* Let us start assuming that  $G$  is a tree, then it is clear from Lemma 4.5 (i) that  $G$  is either  $D_n$  or  $A_n$ . Now, from Lemma 4.5 (iii) we know that  $G$  cannot have two induced cycles with length  $\geq 4$ , so let  $G$  have exactly one cycle of size  $\geq 4$ , then by the cases 1 and 2 of Proposition 4.1,  $G$  must be either a 1-balloon graph or an  $H$  graph. Finally, consider the case where  $G$  has only cycles of size 3. Then, either  $G$  has exactly one bicycle graph (more than one would contradict (iii) in Lemma 4.5) or it has none. Either way, cases 1 to 3 in the previous proof shows that the resulting graph can only be  $t'$ -equivalent to  $D_n$  or  $A_n$ . □

**Theorem 4.7.** *There exists an algorithm linear in  $E + V$  to detect checkerboard graph links with maximal signature from a checkerboard graph.*

*Proof:* From Corollary 4.6 it is clear that to find out if a checkerboard graph link is isotopic to  $L(D_n)$  (or  $L(A_n)$ ) we need an algorithm to detect a finite list of forbidden minors in the corresponding checkerboard graph, and to detect big

cycles. The former is a linear time complexity problem. For the latter, we want to know if there is more than one innermost big cycle, since a checkerboard graph is planar, the total number of cycles is  $2 - V + E$  where  $V$  and  $E$  are the number of vertices and edges, respectively. Also, the number of big cycles is equal to the number of all cycles minus the number of 3-cycles. Since there is an algorithm linear in  $E$  for finding the number of 3-cycles in a planar graph [11], then, the complexity of detecting  $L(D_n)$  or  $L(A_n)$  is linear in  $E + V$ . Now, using Theorem 3.3 it follows that we can detect checkerboard graph links with maximal signature from a checkerboard graph.  $\square$

## 4.5 E7 graphs

A table of all connected graphs with six vertices can be found in [15], so it is not hard to verify that the graphs in Figure 4.6 form a complete list of checkerboard graphs  $t'$ -equivalent to  $E_6$ . A similar table, but far more extensive, for connected graphs with seven vertices can be found in [14]. The following Figures show a list of 42 checkerboard graphs  $t'$ -equivalent to  $E_7$ , some of them used in the previous sections. Notice that they qualify as linking graphs. Although the list is far from being complete, raises the question whether checkerboard graphs  $t'$ -equivalent to  $E_7$  (or  $E_8$ ) are linking graphs.

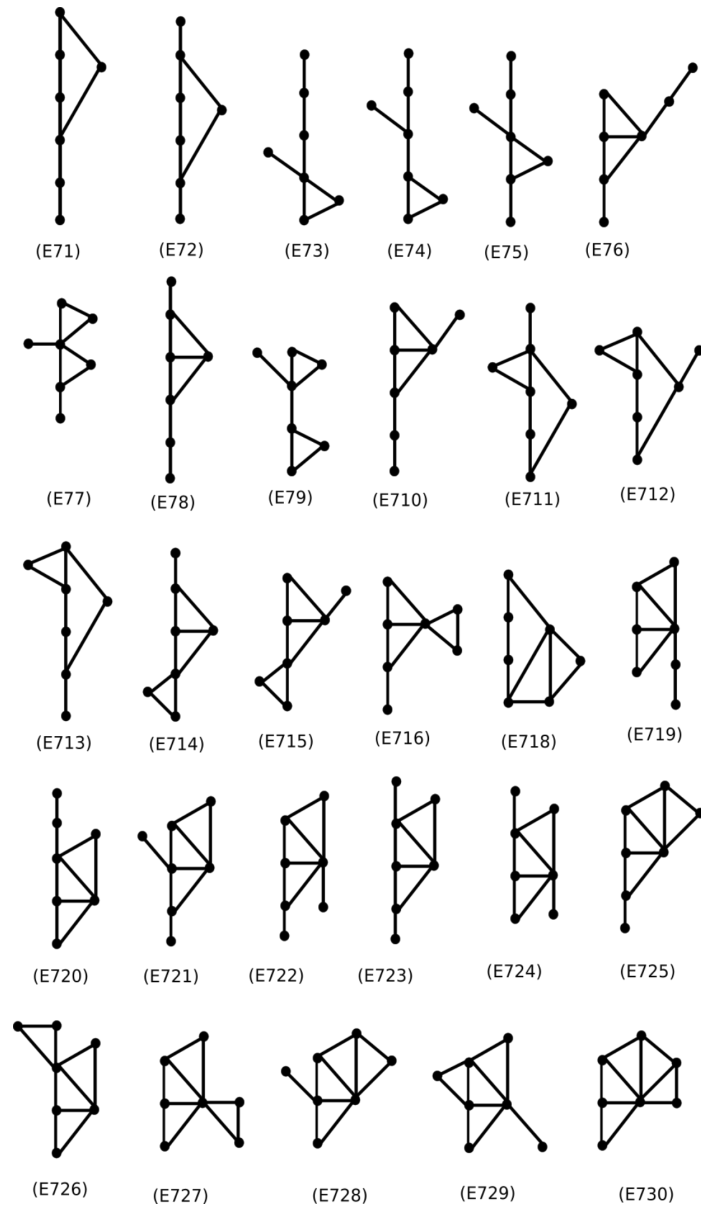


Figure 4.10: List of checkerboard graphs  $t'$ -equivalent to  $E_7$

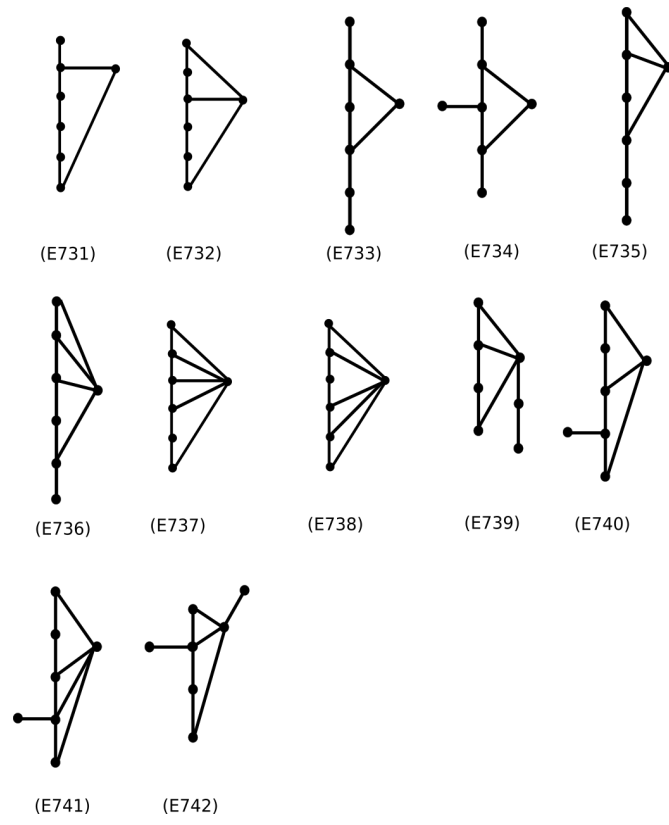


Figure 4.11



## Chapter 5

# Checkerboard graph links and baskets

In this short chapter we will explain how to explicitly construct the link corresponding to the checkerboard graph  $W_n$ , i.e, the  $n$ -wheel graph. Second, we prove that such checkerboard graph links are isotopic to basket links. The motivation is to explore the question whether checkerboard graphs links are basket links.

Given a set of chords in a circle, the intersection graph of these chords is called a circle graph. By [7, Theorem 1.1], the  $W_n$  graphs for  $n = \{6, 8\}$  and  $W_7$  with three non-consecutive rays deleted are circle graph obstructions, and so is any graph that, after a sequence of *local complementation* (we refer the reader to [8] for a definition of local complementation for graphs) contains one of the latter as an induced subgraph. As a result, in [8] they show that  $n$ -wheel graphs for  $n \geq 6$  are not circle graphs. It follows that not every planar graph can be the incidence graph of a basket link, and some of these exceptional graphs, e.g,  $W_n$  for  $n$  odd and  $\geq 9$ , are checkerboard graphs. Note that wheel graphs with an even number of vertices does not admit a checkerboard coloring, so from now on, we consider only wheels with an odd number of vertices. Also, note that the 7-wheel is a linking graph. The question then arises naturally: for  $n \geq 9$  are the checkerboard graphs links arising from  $W_n$  basket links? Here, we show that the answer is yes. In order to prove it, we start with a short explanation of how to construct the link corresponding to the checkerboard graph  $W_n$ , following the construction methods explained in [3]. Second, we find a basket link by sliding bands.

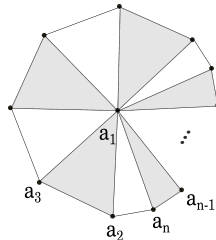


Figure 5.1: A  $W_n$  graph, for  $n$  odd and  $\geq 9$ .

Let  $W_n$  for  $n \geq 9$  be a checkerboard graph. To construct the corresponding checkerboard graph link we will proceed as follows:

First, note that the linking graph with six vertices in Figure 4.6, (6), is an induced subgraph of  $W_n$ . Construct the surface associated with (6) as it is shown in Figure 5.2. Second, plumb the positive Hopf bands  $a_i$  for  $1 \leq i \leq n$  as shown below.

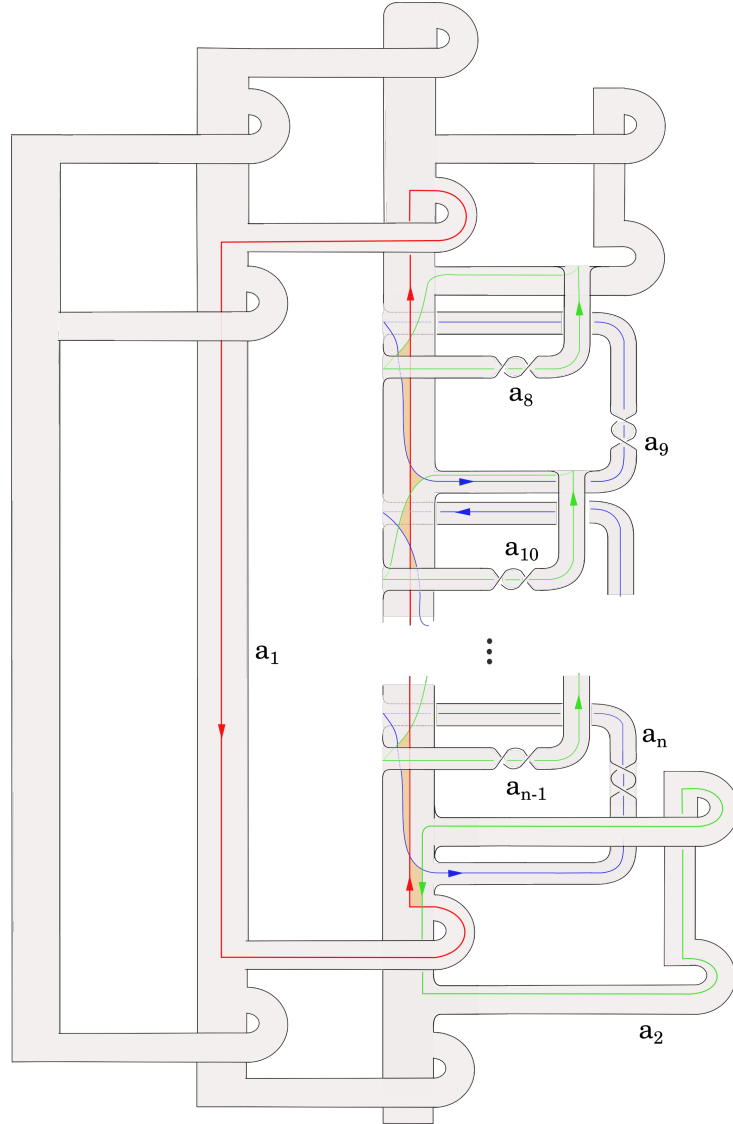


Figure 5.2: The checkerboard graph link corresponding to  $W_n$ .

The result is the same as if we consider the construction method in [3] where the shadow areas represent the disks to be attached. We are now ready to prove the following lemma:



**Lemma 5.1:** *For  $n$  odd and  $\geq 9$ , the checkerboard graph link corresponding to the  $n$ -wheel graph is a basket link.*

*Proof:* Consider the checkerboard graph link corresponding to  $W_9$ , see Figure 5.3, which was constructed using the instructions above. For simplicity, remove the Hopf bands with ends in the shadow areas. Then, slide the bands as indicated. After reattaching the Hopf bands in the shadow areas, the result is a basket link. The same procedure can be easily generalized to  $n > 9$ .  $\square$

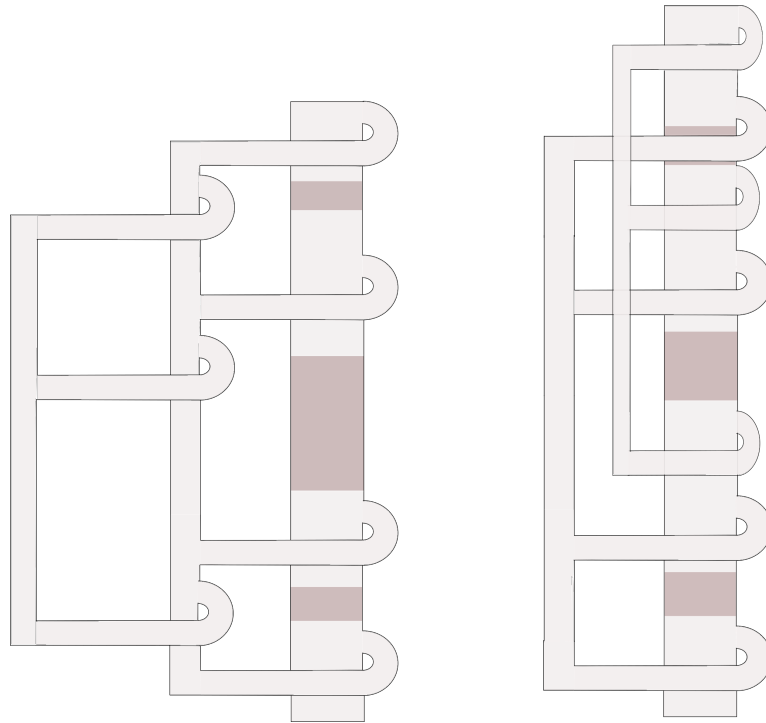


Figure 5.3



## Chapter 6

# Baskets and fibred links realizing $A_n$

This chapter is focused on proving that basket links, whose symmetrized Seifert form is congruent to the Cartan matrix of the simply laced Dynkin diagram  $A_n$ , are isotopic to the torus link  $T(2, n+1)$ . In addition, we provide examples of links, constructed by plumbing  $n$  positive Hopf bands the core curves of which intersect at most once, with symmetrized Seifert form congruent to the Cartan matrix  $A_n$ , that are not isotopic to  $T(2, n+1)$ .

### 6.1 Introduction

The torus links  $T(2, n+1)$  can be constructed by plumbing  $n$  positive Hopf bands according to the diagram  $A_n$  (see Figure 6.1); such construction is an example of what is known as a *positive arborescent Hopf plumbing*. While the congruence class of  $C_{A_n}$  has been studied by graph theorist in the context of the adjacency matrix, see e.g. [22], the links realizing such matrices are far from being understood. As mentioned in the introduction, initial works in this direction show that these are, for some types of links, precisely the two strand torus links  $T(2, n+1)$ . It is the case of positive braids [1], and for certain basket links as pointed out by Boileau et al. [7]. Here, we show that this also works for basket links:

**Theorem 6.1.** *A basket link with  $n$  positive Hopf bands and symmetrized Seifert form congruent to  $C_{A_n}$  is isotopic to a two strand torus link.*

To prove the theorem, in Section 6.2 we show that symmetrized Seifert matrices that are congruent to  $C_{A_n}$  carry a signed graph with a specific structure; they are what we call *complete-tree graphs*. This uses previous results on spectral graph theory and constitutes the first part of the proof of Theorem 6.1. And in Section 6.3, we use this to show by sliding bands, that a basket with such intersection graph is isotopic to a two strand torus link, completing the proof.

Recall that Misev [26] found that there exists an infinite family of distinct

fibred knots having the same Seifert form as the torus knots  $T(2, 2g + 1)$ , for any given genus  $g \geq 2$ . These knots were constructed by plumbing positive Hopf bands such that their core curves intersect more than once. Since for basket links, the core curves of the Hopf bands intersect at most once, this fact together with Theorem 6.1 motivates the question whether we can extend the result of Theorem 6.1. to the more general class of links arising by plumbing positive Hopf bands in which the core curves of the bands intersect at most once.



Figure 6.1: Left: the  $A_n$  diagram. Right: positive Hopf bands plumbed according to the diagram  $A_n$ .

Section 6.3 is dedicated to show, via an example, that this is not true. In the same line as in Misev's article, we show how to construct links and knots with the same Seifert form as the Torus links  $T(2, n + 1)$  but distinct from it. The construction method is to plumb an additional band to a given basket link.

## 6.2 A note on $A_n$ graphs

Graphs whose eigenvalues are larger than  $-2$  have been studied and classified by Cameron et al. in connection with the root systems  $A_n$ ,  $D_n$ ,  $E_6$ ,  $E_7$  and  $E_8$  [9]. A characterization of these graphs was given by Doob and Cvetkovic [13]. Later, Greaves et al. [19] found a similar characterization for signed graphs. In fact, Ishihara [22] shows that the signed graphs of type  $A_n$  come with a specific structure, named *Fushimi trees*. Here, we give an insight in such theories and show an alternative proof to the one of Ishihara.

Let  $G$  be a finite, connected, simple and signed graph. Denote by  $\lambda(G)$  the least eigenvalue of  $A(G)$ , and by  $M(G)$  the matrix  $2I + A(G)$ . If  $\lambda(G) > -2$  we will say that  $G$  is definite.

The root system  $A_n$  is the set of vectors in  $\mathbb{R}^{n+1}$  of the form  $\pm(e_i - e_j)$  for  $1 \leq i < j \leq n + 1$ . A graph  $G$  (signed or not) is said to be represented by a root system if  $M(G) = KK^T$ , where all the rows of  $K$  are vectors in the root system [5]. The line graph of a graph  $G$ , denoted as  $L(G)$ , is a graph in which every vertex represents an edge of  $G$ , and two vertices are adjacent if and only if their corresponding edges share a vertex. For example, the complete graph  $K_n$  is the line graph of a star graph with  $n + 1$  vertices. In [5], they show that a graph is represented by the root system  $A_n$  if and only if it is the line graph of a bipartite

graph. It is not hard to show, that if a graph is signed and represented by  $A_n$ , then its underlying graph is the line graph of a bipartite graph. Denote by  $|G|$  the underlying graph of a signed graph  $G$ .

**Lemma 6.2.** *Let  $G$  be a signed graph such that  $M(G)$  is congruent to  $C_{A_n}$ , then  $|G|$  is the line graph of a tree.*

*Proof:* If  $M(G)$  is congruent to  $C_{A_n}$ , then  $G$  is represented by the root system  $A_n$ , meaning that  $|G| = L(S)$  for a bipartite graph  $S$ . Now, since the line graph of an  $n$ -cycle is again a  $n$ -cycle, if  $S$  has an even cycle, then so does  $|G|$ , but then  $M(G)$  is not congruent to  $C_{A_n}$  as we saw in Chapter 3, independently of the signs. Therefore,  $S$  must be a tree.  $\square$

For simplicity, we will call a signed and definite graph of type  $L(T)$ , for some tree  $T$  by *complete-tree graphs* (or *Fushimi trees*). Note that, switching the signs of the edges incident to a given vertex of a graph,  $G$ , does not change the congruence class of  $M(G)$ . Two signed graphs are *switching equivalent* if we can transform one into another by switching signs without changing the congruence class. It is worth mentioning, that a complete-tree graph is switching equivalent to a complete-tree graph with only positive edges, see [22].

## 6.3 Proof of Theorem 6.1.

As proved by [7] Theorem 9.11, definite graphs of type  $A_n$  and  $K_m$  have a unique realization as baskets. Indeed, they show how these two baskets (when  $n = m$ ) are isotopic by sliding bands. Complete-tree graphs have a unique realization as baskets as well (they are a tree-like amalgamation of the former). In this section we will prove by induction on the number of complete subgraphs, that baskets realized by a complete-tree graph are isotopic to one with incidence graph  $A_n$ . Here, we will adopt the notation in [7], and we will say that a leg of size  $n$  is an  $A_n$  graph attached at one of its leaves to a vertex of a complete graph, and that a basket is definite when its symmetrized Seifert form is positive definite.

**Lemma 6.3:** *Let  $B_s$  be a definite basket with  $s$  bands, the incidence graph of which is  $K_n$  with  $m \leq n$  legs and  $n > 2$ , then  $B_s$  is isotopic to a basket with incidence graph of type  $A_s$ .*

*Proof:* First, consider the configuration of positive Hopf bands plumbed in the disk  $D$  as it appears in Figure 6.2 (a). In terms of the incidence graph the bands  $b_1, \dots, b_s$  form a leg of size  $s$ . From now on, we assume that the legs extend to the left, the proof works similarly otherwise. Slide  $c$  over  $b_0$  (obtaining the bands in

(b)), then  $c'$  over  $b_1$  and continue in this fashion till sliding it over  $b_{s-1}$ , resulting in (c).

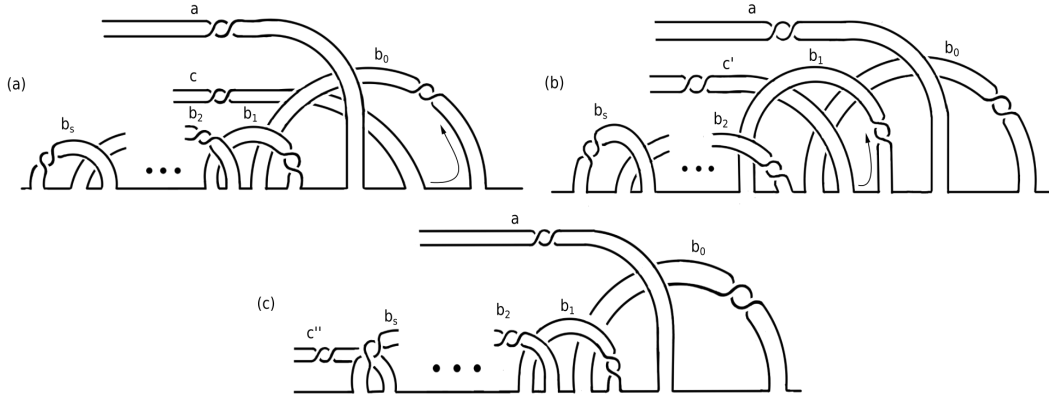


Figure 6.2: Slide  $c$  over  $b_0$  to obtain  $c'$  and repeat.

Now, consider as an example the complete graph  $K_4$  with 4 legs (the cases with less number of legs work similarly) shown in Figure 6.3, where the shadow areas represent where the legs are glued (for simplicity, the legs are not shown in the figure). Note that sliding  $b$  over  $a$  and then sliding it over each of the subsequent bands forming the leg connected to  $a$  (using the moves in Figure 6.2) results in  $K_3$  with 3 legs.  $\square$

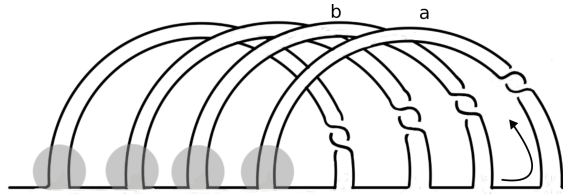


Figure 6.3: The graph  $K_4$  with four legs (represented by the shadow areas). By sliding  $b$  over  $a$  and using the moves in Figure 6.2 we obtain  $K_3$  with three legs.

*Proof of Theorem 6.1:* If a basket link with  $n$  positive Hopf bands has a symmetrized Seifert form congruent to  $C_{A_n}$ , by Lemma 6.2 we know that the incidence graph of such basket is the underlying graph of a complete-tree graph, say  $G$ . We will proceed by induction on the number of complete graphs in  $G$ . Observe that, in  $G$  there is always at least one outermost complete graph with legs, such that the subgraph of  $G$  that results after deleting it, is connected. Since, by Lemma 6.3, the basket with incidence graph the complete graph with legs is isotopic to one with an  $A_n$  incidence graph, the induction follows.  $\square$

## 6.4 Plumbing on a basket

In this section we will explain how to construct links, by plumbing positive Hopf bands with symmetrized Seifert form congruent to  $C_{A_n}$  for  $n \geq 5$  which are not the torus link  $T(2, n+1)$ , and such that the core curves of these Hopf bands intersect at most once. Recall that this differs from the knots studied by Misev [26], where core curves intersect more than once. We consider separately the cases in which  $n$  is odd and even. We will see that the former case are links composed of two components: one of them is the pretzel link  $P(n-3, 1, 1, 1)$  while the other is unknotted.

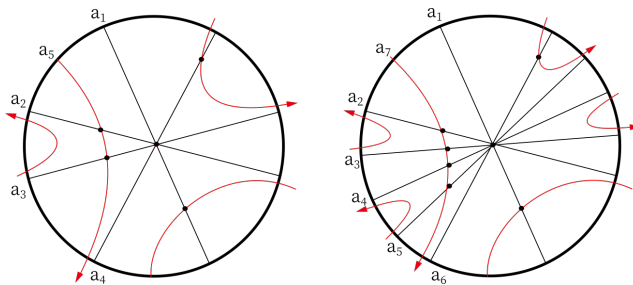


Figure 6.4: Left: Chord diagram with four arcs  $a_1, a_2, a_3, a_4 \subset D_1$  together with a red arc,  $a_5$ , that travels along the Hopf bands indicated with an arrow. Right: an example with seven Hopf bands.

Let us consider the case in which the number of arcs is odd, say  $n = 2m + 1$  for  $m \geq 2$ . Consider a disk  $D \subset \mathbb{R}^2$  with properly embedded arcs  $a_1, \dots, a_{2m}$  (a chord diagram) such that its incidence graph is  $K_{2m}$ . Let  $S_{2m}$  be the surface after plumbing positive Hopf bands on bottom of each other along a neighborhood of the arcs  $a_i$  for  $1 \leq i \leq 2m$ . Let  $\beta$  be a properly embedded arc parallel to  $a_1$  and intersecting all but  $a_1$  (note that there are two equivalent possibilities). Then plumb along the arc  $a_{2m+1} = T_{a_{2m}} \cdots T_{a_2}(\beta)$  (or  $T_{a_2} \cdots T_{a_{2m}}(\beta)$ ), where  $T_a(b)$  stands for the Dehn twist of the curve  $a$  along  $b$ . It is clear that now the core curves of the Hopf bands intersect according to the complete graph  $K_{2m+1}$ . In Figure 6.4 there are two examples of this construction: for five and seven Hopf bands. We can check that the Seifert matrix has congruence type  $A_n$ . In fact, this is easier to check on Figure 6.5.

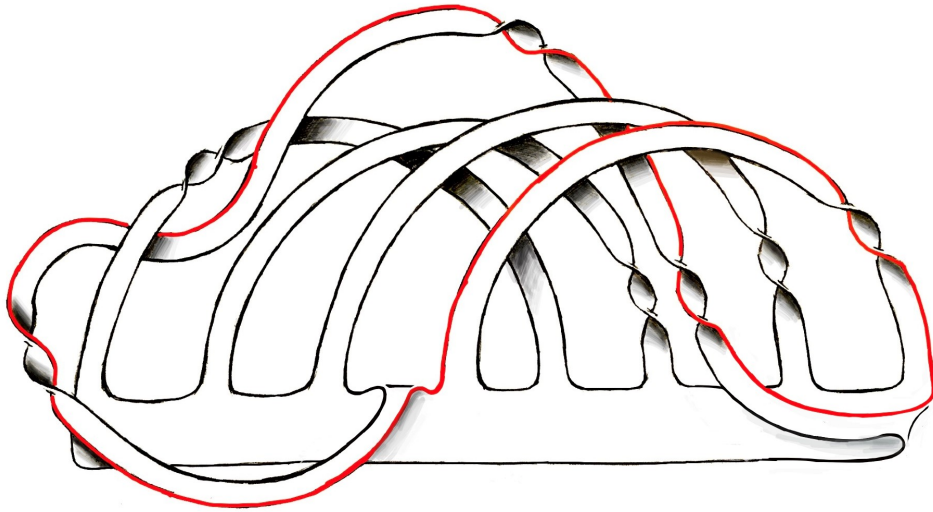


Figure 6.5

We will move our attention to the case with five bands, the resulting surface of which, after isotopy, appears in Figure 6.5. This is a two component link. The linking number is 3 and can be easily computed using Figure 6.5, where one component is marked with red (unknotted!) and the other with black. The latter is the knot  $5_2$ . Therefore, showing that this cannot be the Torus link  $T(2, 6)$ . In order to see this, if we delete the red component, we are left with a rather complicated knot that we have rearranged (using Reidemeister moves) for our convenience as it appears in Figure 6.7, from which is relatively easy to find moves that brings the knot into a recognisable pretzel knot  $P(2, 1, 1, 1)$  (also known as  $5_2$  or  $P(3, 1, 1)$ ). In particular, this shows that this link is not smoothly concordant to  $T(2, 6)$ , since  $5_2$  is not concordant to the unknot. *Snappy* [12] has shown that this is an hyperbolic link, therefore it has a pseudo-Asonov monodromy.

Similarly as we did for the case with five bands, if  $n > 5$ , we still obtain an unknotted component and the other one can be put as in Figure 6.6, from there it is not too hard to obtain the pretzel knots  $P(n - 3, 1, 1, 1)$  in a similar fashion as in Figure 6.7.

The case with six Hopf bands can be obtained using a chord diagram with five arcs and incidence graph  $K_5$ . Let  $\beta$  be an arc intersecting  $a_2$ ,  $a_3$  and  $a_4$  (there are two equivalent possibilities), and plumb the sixth band along  $a_6 = T_{a_4}T_{a_3}T_{a_2}(\beta)$  (or  $a_6 = T_{a_2}T_{a_3}T_{a_4}(\beta)$ ). The resulting knot has 17 crossings (computed with *Knotscape* [21], see Figure 1.4) and its Jones polynomial is different from the one of  $T(2, 7)$ .

**Remark 6.4.** The number of links obtained by positive Hopf plumbing where the core curves intersect at most once is finite. Indeed, by induction, assume that



there are only a finite number of surfaces that can be obtained by plumbing  $n$  positive Hopf bands. Plumb another positive Hopf band to that surface. This must be done along a properly embedded arc in this surface. Now, a result from Przytycki [28] shows that the number of essential simple arcs on a punctured surface with Euler characteristic  $\chi < 0$ , that are pairwise non-homotopic and intersect at most once is exactly  $2|\chi|(|\chi| + 1)$ . The induction follows.

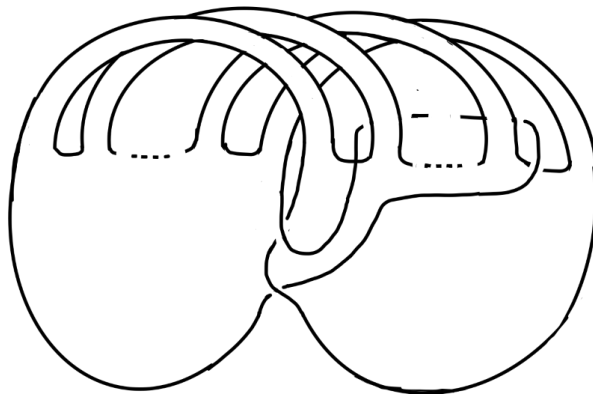


Figure 6.6

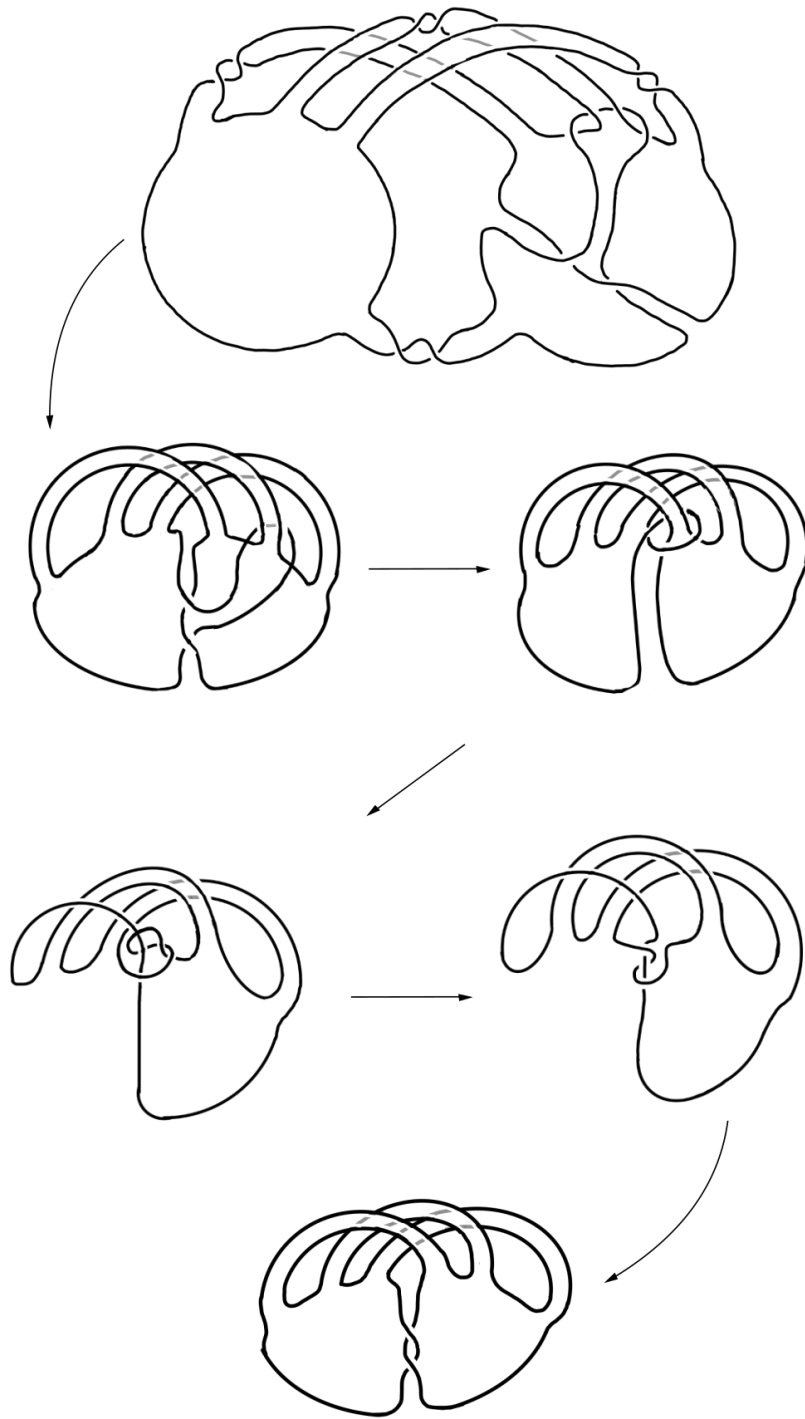


Figure 6.7

# Bibliography

- [1] S. Baader. *Positive braids of maximal signature*. Enseign. Math. **59** (2013), no. 3-4, 351-358.
- [2] S. Baader, L. Lewark. *Positive two strand torus links*. Preprint.
- [3] S. Baader, L. Lewark, L. Liechti. *Checkerboard graph monodromies*. Enseign. Math. **64** (2018), no. 2, 65-88.
- [4] K. L. Baker *A note on the concordance of fibered knots*. Journal of Topology **9** (2016), no. 1, 1-4.
- [5] L. W. Beineke, R. J. Wilson. *Topics in algebraic graph theory*. Encyclopedia of Math. and its Appl. 102, Cambridge University press, Cambridge, 2014, xvi+276pp., ISBN 0-521-80197-4.
- [6] M. Boileau, S. Boyer, C. McA. Gordon. *Branched covers of quasipositive links and L-spaces*. Journal of Topology **12(2)** (2019), 536–576.
- [7] M. Boileau, S. Boyer, C. McA. Gordon. *On definite strongly quasipositive links and L-space branched covers*. Advances of Mathematics, 357 (2019), 106828, 63pp.
- [8] A. Bouchet. *Circle graph obstructions*. Journal of combinatorial theory, Series B **60** (1994), no.1, 107-144.
- [9] P.J. Cameron, J.-M. Goethals, J.J. Seidel, E.E. Shult. *Line graphs, root systems, and elliptic geometry*. Journal of algebra **43** (1976), no. 1, 305-327.
- [10] P.J. Cameron, J.J. Seidel, S. V. Tsaranov. *Signed graphs, root lattices, and Coxeter groups*. Journal of algebra **164** (1994), no.1, 173-209.
- [11] N. Chiba, T. Nishizeki. *Arboricity and subgraph listing algorithms*. Siam J. Comput. **14** (1985), no.1, 210-223.
- [12] M. Culler, N. M. Dunfield, M. Goerner, J. R. Weeks. *SnapPy, a computer program for studying the geometry and topology of 3-manifolds*. <http://snappy.computop.org>.

- [13] D. Cvetković, M. Doob. *On spectral characterizations and embeddings of graphs*. Linear Algebra and its Applications **27** (1979), 17-26.
- [14] D. Cvetković, M. Doob, I. Gutman, A. Torgašev. *Recent results in the theory of graph spectra*. North-Holland, Amsterdam (1988).
- [15] D. Cvetković, M. Petrić. *A table of connected graphs on six vertices*. Discrete Mathematics **50** (1984), 37-49.
- [16] P. Dehornoy. *On the zeros of the Alexander polynomial of a Lorenz knot*. Annals de l'Institut Fourier **65** (2015), no.2, 509-548.
- [17] Susanna S. Epp. *Discrete mathematics with applications*. Brooks/Cole Publishing Co.Div. of International Thomson Publ. Co. 511 Forrest Lodge Road Pacific Grove, CA, United States, ISBN 978-0-495-39132-6.
- [18] E. Giroux, N. Goodman. *On the stable equivalence of open books in three-manifolds*. Geom. Topol. **10** (2006), 97-114.
- [19] G. Greaves, J. Koolen, A. Munemasa, Y. Sano, T. Taniguchi. *Edge-signed graphs with smallest eigenvalue greater than  $-2$* . J. of Combinatorial Theory, Series B **110** (2015), 90-111.
- [20] E. Hironaka. *Chord diagrams and Coxeter links*. J. London Math. Soc. **69** (2004), no. 1, 243-257.
- [21] J. Hoste, M. Thistlethwaite. *KnotScape, a knot polynomial calculation program*. <http://www.math.utk.edu/~morwen/knotscape.html>, 1999.
- [22] T. Ishihara. *Signed graphs associated with the lattice  $A_n$* . J. Math. Univ. Tokushima **36** (2002), 1-6.
- [23] J. Levine. *Invariants of knot cobordism*. Inventiones Math. **8** (1969), 98-110.
- [24] L. Liechti. *Positive braid knots of maximal topological 4-genus*. Math. Proc. Cambridge Philos. Soc. **161** (2016), no. 3, 559-568.
- [25] P. M. Melvin, H. R. Morton. *Fibred knots of genus 2 formed by plumbing Hopf bands*. J. London Math. Soc.(2) **34** (1986), no. 1, 159-168.
- [26] F. Misev. *On families of fibred knots with equal Seifert forms*. arXiv:1703.07632v1 (2017).
- [27] K. Murasugi. *On a certain subgroup of the group of an alternating link*. Amer. J. Math. **85** (1963), no. 4, 544-550.
- [28] P. Przytycki. *Arcs intersecting at most once*. Geom. Funct. Anal. **25** (2015), no. 2, 658-670.

- [29] D. Rolfsen. *Knots and links*. Mathematics Lecture Series, vol. 7. Publish or Perish Inc, Houston (1990).
- [30] L. Rudolph. *Hopf plumbing, arborescent Seifert surfaces, baskets, espaliers, and homo-geneous braids*. Topology Appl. **116(3)** (2001), 255-277.
- [31] J. R. Stallings. *On fibering certain 3-manifolds*. Topology of 3-manifolds and related topics, Proc. Univ. Georgia Inst. (1961), Prentice-Hall, Englewood Cliffs, N.J., 95-100.
- [32] J. R. Stallings. *Constructions of fibred knots and links*. Algebraic and geometric topology, Proc. Sympos. Pure Math. **32** (1978), Part 2, 55-60, Amer. Math. Soc., Providence, R.I.
- [33] A. G. Tristram. *Some cobordism invariants for links*. Proc. Camb. Phil. Soc. **66** (1969), 251-264.
- [34] H. F. Trotter. *Homology of group systems with applications to knot theory*. Annals of Mathematics **76** (1962), no.3, 464-498.



## Declaration of consent

on the basiss of Article 18 of the PromR Phil.-nat. 19

Name/First Name: Fernandez Vilanova Lucas

Registration Number: 16-126-146

Study Program: Dissertation

Title of the thesis: Positive Hopf plumbed links with maximal signature

Supervisor: Prof. Dr. Sebastian Baader

I declare herewith that this thesis is my own work and that I have not used any sources other than those stated. I have indicated the adoption of quotations as well as thoughts taken from other authors as such in the thesis. I am aware that the Senate pursuant to Article 36 paragraph 1 litera r of the University Act of September 5th, 1996 and Article 69 of the University Statute of June 7th, 2011 is authorized to revoke the doctoral degree awarded on the basis of this thesis. For the purposes of evaluation and verification of compliance with the declaration of originality and the regulations governing plagiarism, I hereby grant the University of Bern the right to process my personal data and to perform the acts of use this requires, in particular, to reproduce the written thesis and to store it permanently in a database, and to use said database, or to make said database available, to enable comparison with theses submitted by others.

Bern, 17. December 2020

Lucas Fernandez Vilanova